Nuclear Physics A408 (1983) 425–460

EXCHANGE EFFECTS IN PHOTON SCATTERING OFF THE DEUTERON†

M. WEYRAUCH and H. ARENHÖVEL

Institut für Kernphysik, Johannes Gutenberg-Universität, D-6500 Mainz, Federal Republic of Germany

Received 10 March 1983

Abstract: Detailed calculations of elastic photon–deuteron scattering cross sections for photon energies up to about the π-production threshold are presented. The scattering amplitude is decomposed into scalar, vector and tensor polarizabilities for the various electric and magnetic multipole combinations. This includes a general multipole expansion of the two-photon operator. The imaginary part of the polarizabilities is determined from the contribution to the total cross section using the optical theorem. The real part is then obtained from dispersion relations. Special emphasis is laid on the discussion of exchange effects for both the resonance and the two-photon amplitude. These affect strongly the resonance amplitude whereas for the two-photon amplitude we find only a small effect beyond the important low-energy limit. Another important result is the large vector polarizability at higher energies related to the optical activity of the deuteron.

1. Introduction

A potentially rich tool to investigate the structure of nuclei is provided by photon scattering since, firstly, the whole nuclear dynamics is involved in the scattering process and, secondly, due to the electromagnetic nature of the interaction a clear interpretation of experimental data is possible. Furthermore, the scattering process gives supplementary information with respect to photoabsorption processes to which it is linked by the optical theorem.

Past activities in this field have concentrated mainly on the low-energy region up to the giant dipole resonance in order to study spectroscopic properties, excitation of collective degrees of freedom as well as quantum electrodynamic processes like Delbrück scattering. Recently that has been nicely reviewed by Moreh [1]). For other reviews see refs. [2,3]). Besides these more conventional nuclear structure problems there is now increasing interest in the rôle of non-nucleonic degrees of freedom like meson exchange (MEC) and isobar currents (IC) in nuclear photon scattering [4–8]).

An important observation with respect to two-photon processes like photon scattering is the fact that here meson-exchange corrections enter twice, first as two-body currents in the resonance amplitude and second as genuine exchange

† Partially supported by the Deutsche Forschungsgemeinschaft (SFB 0201).

two-photon amplitudes (ETPA). Both are required to ensure gauge invariance, a point which is discussed in detail in refs. [4,6,8]).

Whereas the effects of MEC and IC have been extensively studied in "one-photon processes", e.g. photoabsorption or electron scattering [9,10]), much less effort has been devoted to meson-exchange corrections in two-photon processes such as photon scattering, two-photon decays or dispersion corrections in electron scattering. Explicit expressions of ETPA have been derived in the one-pion-exchange approximation along different lines in refs. [5,8]). An application of these amplitudes using their low-energy limit is discussed by Cambi *et al.* [11]) considering M1–M1 transitions in doubly radiative n-p capture. They find in this case a very small contribution of ETPA to this process.

The importance of meson-exchange corrections in nuclear photon scattering has been stressed in a series of papers by Christillin and Rosa-Clot [6,7]). They estimated using low-energy theorems that exchange effects strongly influence the scattering amplitude above the giant resonance region and below pion production threshold. However, concerning the low-energy region it was found that MEC and ETPA do not explicitly influence the scattering amplitude [4,8]), if one uses as usual Siegert's theorem evaluating the current matrix elements for the resonance amplitude and the proper low-energy expression for the two-photon amplitude. Therefore, the interesting region to investigate such two-photon contributions is certainly the region beyond the giant dipole region up to and above the pion production threshold.

Unfortunately, there is little experimental information concerning the importance of meson-exchange corrections in the nuclear two-photon amplitude from photon scattering. This is obviously due to the enormous experimental difficulties in this field. Only recently, the influence of exchanged mesons on the TPA has been studied by Ziegler and collaborators in photon scattering experiments on ^{208}Pb [ref. [12])] and ^{181}Ta [ref. [13])]. In fact, some evidence of exchange effects in the TPA has been found. But the actual size is not clear because of lack of information on the angular distribution and on the multipole decomposition of the total photoabsorption cross section which is used as input for the resonance amplitude. Furthermore, various phenomenological models for ETPA have been used in that analysis.

As already mentioned, existing evaluations of the ETPA for photon scattering have used extrapolations of the low-energy theorems which seem to be doubtful. It seems, therefore, timely to study these effects avoiding such approximations. To this end, we will first formally derive the contribution of the most important one-pion ETPA to the nuclear polarizabilities into which the photon scattering amplitude is expanded. These results will then be used to calculate ETPA contributions to elastic photon deuteron scattering. As has been pointed out already in ref. [9]) a shortcoming of the usual static meson-exchange models is the fact that they do not describe the real meson production channel for excitation energies above meson production threshold. Therefore, the quantitative results presented in this paper are limited to energies below pion production threshold.

Besides the TPA we need to evaluate also the resonance amplitude in order to have a complete description of the photon scattering process. Since this is a second-order process one has to sum in principle over all intermediate states. Various methods have been developed to overcome this problem. In the discussion of dispersion corrections in electron scattering the closure approximation is often used for summing over intermediate states in replacing the energy denominators by a suitably chosen average value [14]). Another method is to approximate the set of intermediate states by a few, but important states which are dominantly excited and represent them by Lorentz lines [15,16]).

The use of dispersion relations in connection with the optical theorem is another, in principle, exact tool. The latter relates the absorption cross section to the imaginary part of the elastic scattering amplitude in the forward direction, while disperion relations connect the imaginary and the real part of the scattering amplitude [17]). We will use the last approach, which seems to be especially suited for our problem of discussing deuteron photon scattering. A new feature will be the use of dispersion relations for the separate polarizabilities allowing the calculation of angular distributions. Since we have not included the channels for real pion production the calculated resonance amplitude will fail approaching the pion production threshold.

In sect. 2 we will review the general structure of the photon scattering amplitude defining our conventions and notations. In sect. 3 we will derive the decomposition of the two-photon amplitude and of the resonance amplitude in terms of nuclear polarizabilities. Applications of these results on deuteron photon scattering are discussed in the last section. Calculational details will be presented in appendices. (We use gaussian units and $\hbar = c = 1$.)

2. Basic results of photon scattering theory

Let us first review some basic formulas needed for the description of nuclear photon scattering. A photon with energy and momentum $(k, \boldsymbol{k})$ and polarization $\boldsymbol{\varepsilon}_\lambda$ is scattered off a nucleus with energy and momentum $(E_i, \boldsymbol{P}_i)$. The scattered photon emerges with energy and momentum $(k', \boldsymbol{k}')$ and polarization $\boldsymbol{\varepsilon}'_{\lambda'}$ leaving the nucleus in a state with energy and momentum $(E_f, \boldsymbol{P}_f)$. Taking the interaction of the nucleus with the radiation field up to second order in the electromagnetic potential $\boldsymbol{A}(\boldsymbol{x})$,

$$H_{\text{e.m.}}(\boldsymbol{A}) = -\int \mathrm{d}^3x\, \boldsymbol{j}(\boldsymbol{x}) \cdot \boldsymbol{A}(\boldsymbol{x}) + \tfrac{1}{2} \sum_{l',l} \int \mathrm{d}^3x\, \mathrm{d}^3y\, A_{l'}(\boldsymbol{x}) B_{l'l}(\boldsymbol{x}, \boldsymbol{y}) A_l(\boldsymbol{y}) , \tag{1}$$

then in second-order perturbation theory the T-matrix is given by

$$T^{\text{fi}}_{\lambda'\lambda}(\boldsymbol{k}', \boldsymbol{k}) = B^{\text{fi}}_{\lambda'\lambda}(\boldsymbol{k}', \boldsymbol{k}) + T^{\text{fi,res}}_{\lambda'\lambda}(\boldsymbol{k}', \boldsymbol{k}) . \tag{2}$$

Here the first term is the first-order contribution of the two-photon-operator $B_{l'l}$

of eq. (1), and the second term, the resonance amplitude, describes the contribution of the current density operator in second order. Explicitly one has

$$B^{\mathrm{fi}}_{\lambda'\lambda}(\boldsymbol{k}',\boldsymbol{k}) = -\langle \mathrm{f}| \int \mathrm{d}^3x\,\mathrm{d}^3y\,\mathrm{e}^{-i\boldsymbol{k}'\cdot\boldsymbol{x}}\,\mathrm{e}^{i\boldsymbol{k}\cdot\boldsymbol{y}} \sum_{l',l} \varepsilon^{\prime *}_{\lambda',l'} B_{l'l}(\boldsymbol{x},\boldsymbol{y})\varepsilon_{\lambda,l}|\mathrm{i}\rangle\,. \tag{3}$$

Note that sometimes a different sign convention for T has been used, e.g. in refs. [4,6,8]). Translation invariance has been used to separate out the c.m. motion. Therefore $|\mathrm{i}\rangle$ and $|\mathrm{f}\rangle$ refer to the initial and final intrinsic nuclear states. The resonance amplitude is given by

$$\begin{aligned} T^{\mathrm{fi}}_{\lambda'\lambda}(\boldsymbol{k}',\boldsymbol{k}) = &\sum_n \frac{\langle \mathrm{f}|\boldsymbol{\varepsilon}^{\prime *}_{\lambda'}\cdot\tilde{\boldsymbol{j}}(-\boldsymbol{k}',2\boldsymbol{P}_{\mathrm{f}}+\boldsymbol{k}')|n\rangle\langle n|\boldsymbol{\varepsilon}_{\lambda}\cdot\tilde{\boldsymbol{j}}(\boldsymbol{k},2\boldsymbol{P}_{\mathrm{i}}+\boldsymbol{k})|\mathrm{i}\rangle}{E_n-E_{\mathrm{i}}-k-i\varepsilon} \\ &+\sum_n \frac{\langle f|\boldsymbol{\varepsilon}_{\lambda}\cdot\tilde{\boldsymbol{j}}(\boldsymbol{k},2\boldsymbol{P}_{\mathrm{f}}-\boldsymbol{k})|n\rangle\langle n|\boldsymbol{\varepsilon}^{\prime *}_{\lambda'}\cdot\tilde{\boldsymbol{j}}(-\boldsymbol{k}',2\boldsymbol{P}_{\mathrm{i}}-\boldsymbol{k}')|\mathrm{i}\rangle}{E_n-E_{\mathrm{i}}+k'-i\varepsilon}\,, \end{aligned} \tag{4}$$

where

$$\langle \mathrm{f}|\tilde{\boldsymbol{j}}(\boldsymbol{k},\boldsymbol{P})|\mathrm{i}\rangle = \langle \mathrm{f}|\int \mathrm{d}^3x\,\tilde{\boldsymbol{j}}(\boldsymbol{x})\,\mathrm{e}^{i\boldsymbol{k}\cdot\boldsymbol{x}} + \frac{\boldsymbol{P}}{2AM}\int \mathrm{d}^3x\,\tilde{\rho}(\boldsymbol{x})\,\mathrm{e}^{i\boldsymbol{k}\cdot\boldsymbol{x}}|\mathrm{i}\rangle\,. \tag{5}$$

The tilde on the charge and current density operators in eqs. (4) and (5) indicates, that these operators refer to intrinsic coordinates and momenta, since the c.m. motion has been separated already. The second term in eq. (5) is the convection current contribution of the c.m. motion. It is small for not too high energies and will be neglected in the explicit evaluation. The energies E_{i} and E_n in eq. (4) denote initial and intermediate total energy of the nucleus including the c.m. energy, e.g.

$$E_{\mathrm{i}} = \varepsilon_{\mathrm{i}} + \boldsymbol{P}_{\mathrm{i}}^2/2AM\,, \tag{6}$$

where ε_{i} is the energy of the intrinsic nuclear motion with respect to the c.m. system.

For convenience we will write the resonance amplitude in a form similar to eq. (3) by introducing the operator

$$T^{\mathrm{res}}_{l'l}(\boldsymbol{x},\boldsymbol{y}) = t_{l'l}(\boldsymbol{x},\boldsymbol{y},\boldsymbol{k},k+i\varepsilon) + t_{ll'}(\boldsymbol{y},\boldsymbol{x},-\boldsymbol{k}',-k'+i\varepsilon)\,, \tag{7}$$

where

$$t_{l'l}(\boldsymbol{x},\boldsymbol{y},\boldsymbol{k},k) = \left(\tilde{j}_{l'}(\boldsymbol{x}) + \frac{P_{\mathrm{f},l'}}{AM}\tilde{\rho}(\boldsymbol{x})\right)\left(H_0 + \frac{(\boldsymbol{P}_{\mathrm{i}}+\boldsymbol{k})^2}{2AM} - E_{\mathrm{i}} - k\right)^{-1}\left(\tilde{j}_l(\boldsymbol{y}) + \frac{P_{\mathrm{i},l}}{AM}\tilde{\rho}(\boldsymbol{y})\right). \tag{8}$$

Here H_0 refers to the intrinsic hamiltonian. Then we have for the total amplitude

$$T^{\mathrm{fi}}_{\lambda'\lambda}(\boldsymbol{k}',\boldsymbol{k}) = \langle \mathrm{f}|\int \mathrm{d}^3x\,\mathrm{d}^3y\,\mathrm{e}^{-i\boldsymbol{k}'\cdot\boldsymbol{x}+i\boldsymbol{k}\cdot\boldsymbol{y}} \sum_{l',l} \varepsilon^{\prime *}_{\lambda',l'} T_{l',l}(\boldsymbol{x},\boldsymbol{y})\varepsilon_{\lambda,l}|\mathrm{i}\rangle\,, \tag{9}$$

where

$$T_{l'l}(\boldsymbol{x},\boldsymbol{y}) = -B_{l'l}(\boldsymbol{x},\boldsymbol{y}) + T^{\mathrm{res}}_{l'l}(\boldsymbol{x},\boldsymbol{y})\,. \tag{10}$$

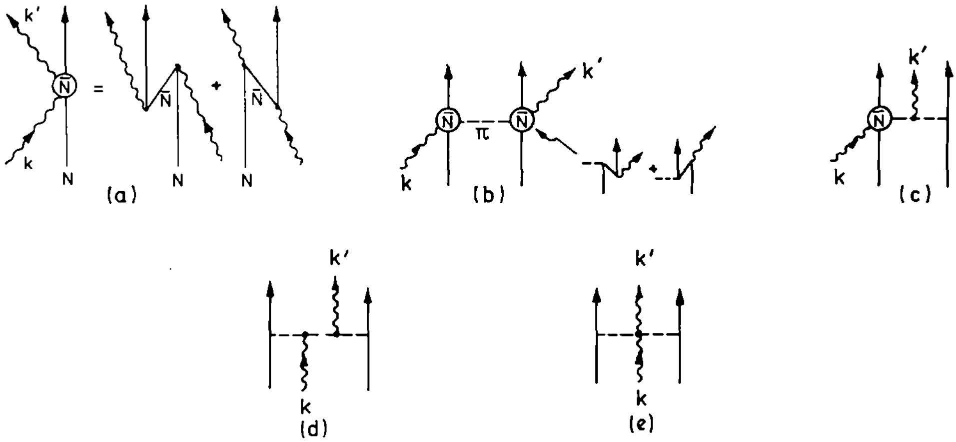

Fig. 1. Diagrams of the kinetic (a) and π-exchange ((b)–(e)) two-photon amplitudes.

It is important to note that the current and charge operators $\boldsymbol{j}(\boldsymbol{x})$, $\rho(\boldsymbol{x})$ and the two-photon operator $B_{l'l}(\boldsymbol{x}, \boldsymbol{y})$ are not independent, but are related by the gauge condition

$$\frac{\partial}{\partial x_{l'}} B_{l'l}(\boldsymbol{x}, \boldsymbol{y}) = i[\rho(\boldsymbol{x}), j_l(\boldsymbol{y})], \tag{11}$$

as discussed in detail in refs. [4,6,8]).

Let us now discuss the various terms of the amplitude (2). First we have the two-photon amplitude, which arises if the electromagnetic interaction hamiltonian contains quadratic terms in the vector potential $\boldsymbol{A}$. Such terms are always generated in minimal coupling, if the nuclear hamiltonian depends on some momentum variables quadratically as e.g. in a non-relativistic theory the contribution due to the kinetic energy operator

$$B^{\mathrm{fi,kin}}_{\lambda'\lambda}(\boldsymbol{k}', \boldsymbol{k}) = -\frac{\boldsymbol{\varepsilon}'^{*}_{\lambda'} \cdot \boldsymbol{\varepsilon}_{\lambda}}{M} \langle \mathrm{f} | \sum_j e_j^2 \, \mathrm{e}^{i(\boldsymbol{k}-\boldsymbol{k}')\cdot \boldsymbol{r}_j} | \mathrm{i} \rangle , \tag{12}$$

which is shown diagrammatically in fig. 1a. It describes Thomson scattering off the individual particles. The coordinates $\boldsymbol{r}_j$ refer to relative coordinates with respect to the center of mass.

We would like to mention, that for a Dirac particle the kinetic two-photon amplitude is absent. It arises in the non-relativistic reduction as contribution of the resonance term with intermediate antiparticle states. The kinetic two-photon operator fulfills the condition

$$\frac{\partial}{\partial x_{l'}} B^{\mathrm{kin}}_{l'l}(\boldsymbol{x}, \boldsymbol{y}) = i[\rho_{(1)}(\boldsymbol{x}), \boldsymbol{j}_{(1)l}(\boldsymbol{y})], \tag{13}$$

with the one-body charge and current densities

$$\rho_{(1)}(\boldsymbol{x}) = \sum_j e_j \delta(\boldsymbol{x} - \boldsymbol{r}_j) = \sum_j \rho_{(1)j}, \tag{14}$$

$$\boldsymbol{j}_{(1)}(\boldsymbol{x}) = \frac{1}{2M} \sum_j \{\boldsymbol{p}_j, \rho_{(1)j}\}. \tag{15}$$

With respect to the gauge condition (11) it is obvious that another contribution to the two-photon operator ($B_{l'l}^{\text{MEC}}$) arises if exchange forces are present. Because in this case the one-body current (15) has to be supplemented by a two-body exchange current $\boldsymbol{j}_{(2)}^{\text{MEC}}$ and then (11) is not fulfilled with $B_{l'l}^{\text{kin}}$ alone. In view of (13) one then has as gauge condition for $B_{l'l}^{\text{MEC}}$

$$\frac{\partial}{\partial x_{l'}} B_{l'l}^{\text{MEC}}(\boldsymbol{x}, \boldsymbol{y}) = i[\rho_{(1)}(\boldsymbol{x}), j_{(2)l}^{\text{MEC}}(\boldsymbol{y})], \tag{16}$$

assuming that no two-body contribution to the charge density exists (Siegert hypothesis).

In the case of the one-pion exchange potential (OPEP) the related two-photon amplitudes have been derived explicitly [5,8]) and the corresponding diagrams are shown in figs. 1b–e. These contributions arise from the exclusion of explicit meson degrees of freedom and describe in essence resonance contributions with intermediate production of virtual pions (figs. 1b, c) as well as resonance and Thomson scattering off an exchanged meson (figs. 1d, e).

The inclusion of intermediate excitation of anti-nucleon resonances (e.g. $\bar{\Delta}$) leads to additional contributions to the two-photon amplitude, but will not be considered in this paper because they are expected to be small in the energy region we are considering here [8]).

The next term in (2) is the so-called resonance contribution. It describes photon scattering as a two-step process via intermediate excitation of the nucleus (see fig. 2). The nuclear currents $\boldsymbol{j}(\boldsymbol{k})$ are determined by one-body currents of the nucleons and by two-body contributions of the exchanged mesons (MEC). The calculation of the resonance amplitude is rather cumbersome, because in principle one has to sum over all nuclear excitations weighted with the appropriate energy denominators. As already mentioned in the introduction, we will use a dispersion theoretical approach for solving this problem, which will be described in the next section.

We would like to emphasize once more that the various parts of (2) are not independent, but are related by gauge conditions. One important consequence is, for example, the well-known low-energy theorem, which states that the photon scattering amplitude for k, $k' \to 0$ is given by the classical Thomson amplitude

$$T_{\lambda'\lambda}^{\text{ii}}(0, 0) = -\boldsymbol{\varepsilon}_{\lambda'}^{\prime *} \cdot \boldsymbol{\varepsilon}_\lambda \frac{Z^2 e^2}{AM}. \tag{17}$$

The separate contributions of the resonance and two-photon amplitudes to this

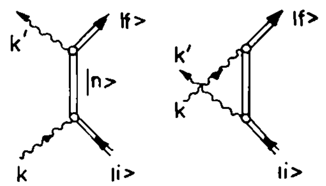

Fig. 2. Diagrams for the resonance amplitude.

low-energy limit are given by [8])

$$B^{\text{ii,kin}}_{\lambda'\lambda}(0,0) = -\boldsymbol{\varepsilon}'^{*}_{\lambda'} \cdot \boldsymbol{\varepsilon}_{\lambda} \frac{Ze^2}{M}, \tag{18}$$

$$B^{\text{ii,MEC}}_{\lambda'\lambda}(0,0) = -\langle \mathrm{i}|[\boldsymbol{\varepsilon}'^{*}_{\lambda'} \cdot \boldsymbol{D}, [V, \boldsymbol{\varepsilon}_{\lambda} \cdot \boldsymbol{D}]]|\mathrm{i}\rangle, \tag{19}$$

$$\begin{aligned} T^{\text{ii,res}}_{\lambda'\lambda}(0,0) &= \langle \mathrm{i}|[\boldsymbol{\varepsilon}'^{*}_{\lambda'} \cdot \boldsymbol{D}, [H_0, \boldsymbol{\varepsilon}_{\lambda} \cdot \boldsymbol{D}]]|\mathrm{i}\rangle \\ &= \boldsymbol{\varepsilon}'^{*}_{\lambda'} \cdot \boldsymbol{\varepsilon}_{\lambda} \frac{NZ}{A}\frac{e^2}{M} + \langle \mathrm{i}|[\boldsymbol{\varepsilon}'^{*}_{\lambda'} \cdot \boldsymbol{D}, [V, \boldsymbol{\varepsilon}_{\lambda} \cdot \boldsymbol{D}]]|\mathrm{i}\rangle . \end{aligned} \tag{20}$$

The double commutator of the dipole operator with the potential in eq. (19) describes also the enhancement of the photonuclear TRK sum rule. This illustrates the importance of the exchange two-photon amplitude, which is necessary to cancel the corresponding contribution in the resonance amplitude in order to fulfil the low-energy theorem.

In closing this section we give the differential cross section in the lab system

$$\left(\frac{\mathrm{d}\sigma}{\mathrm{d}\Omega}\right)_{\mathrm{L}} = \frac{k'_{\mathrm{L}}}{k_{\mathrm{L}}} |T^{\mathrm{fi}}_{\lambda'\lambda}(\boldsymbol{k}', \boldsymbol{k})|^2, \tag{21}$$

where k_{L} and k'_{L} are related by the Compton formula

$$k'_{\mathrm{L}} = \frac{k_{\mathrm{L}} - \Delta}{1 + k_{\mathrm{L}}(1 - \cos\theta_{\mathrm{L}})/M_0}, \tag{22}$$

with $\Delta = (M_{\mathrm{f}}^2 - M_0^2)/2M_0$. We have denoted the nuclear ground- and final-state mass by M_0 and M_{f}, respectively, and the scattering angle in the lab system by θ_{L}.

For the explicit calculation of the elastic cross section the Breit frame will be more useful, because then one has

$$\boldsymbol{p}_{\mathrm{i}}^{\mathrm{B}} = -\boldsymbol{p}_{\mathrm{f}}^{\mathrm{B}}, \qquad k_{\mathrm{B}} = k'_{\mathrm{B}}, \tag{23}$$

and the cross section is simply given by

$$\left(\frac{\mathrm{d}\sigma}{\mathrm{d}\Omega}\right)_{\mathrm{B}} = |T^{\mathrm{fi}}_{\lambda'\lambda}(\boldsymbol{k}', \boldsymbol{k})|^2 . \tag{24}$$

The jacobian relating the Breit frame to the lab frame cross section is given by

$$\frac{\mathrm{d}\Omega_\mathrm{B}}{\mathrm{d}\Omega_\mathrm{L}}=\frac{k'_\mathrm{L}}{k'_\mathrm{B}}\frac{E_\mathrm{i}^\mathrm{B}}{M_0}\left(1+\frac{p_\mathrm{i}^\mathrm{B}}{E_\mathrm{i}^\mathrm{B}}\sin\left(\tfrac{1}{2}\theta_\mathrm{B}\right)\right), \tag{25}$$

where

$$k_\mathrm{B}=(k_\mathrm{L}+k'_\mathrm{L})(2(2M_0+k_\mathrm{L}-k'_\mathrm{L})/M_0)^{1/2}, \tag{26}$$

$$\cos\theta_\mathrm{B}=1-(1-\cos\theta_\mathrm{L})k_\mathrm{L}k'_\mathrm{L}/k_\mathrm{B}^2, \tag{27}$$

$$E^\mathrm{B}=(M_0^2+M_0(k_\mathrm{L}-k'_\mathrm{L})/2)^{1/2}, \qquad p_\mathrm{i}^\mathrm{B}=((E_\mathrm{i}^\mathrm{B})^2-M_0^2)^{1/2}. \tag{28}$$

Here the sub- or superscripts B and L indicate Breit and lab frame quantities. For the present application to photon-deuteron scattering and energies below 200 MeV the jacobian is almost unity.

3. Nuclear polarizabilities

A useful concept for the description of photon scattering is given by the generalized nuclear polarizabilities [16,18]) corresponding to an expansion of the scattering amplitude in terms of the total angular momentum transferred to the target nucleus. It allows a clean separation of the dynamical and geometrical properties of the system. Each of the absorbed and emitted photons transfers angular momentum and parity, i.e. electric or magnetic multipole of order L and L', respectively, and as a consequence one can decompose the scattering amplitude according to the angular momentum transferred and to the type of multipoles involved (see fig. 3).

Since in previous work this decomposition has been done essentially for the resonance part only, because the two-photon amplitude has been taken in the low-energy limit, we will sketch it briefly for the general case including the two-photon amplitude. The starting point is the multipole expansion of the plane wave

$$\boldsymbol{\varepsilon}_\lambda\,\mathrm{e}^{i\boldsymbol{k}\cdot\boldsymbol{x}}=-\sqrt{2\pi}\sum_{\substack{L,M\\ \nu=0,1}}\hat{L}\lambda^\nu\boldsymbol{A}^{[L],M}(M^\nu;k)D^L_{M,\lambda}(R), \qquad \hat{L}=\sqrt{2L+1}, \tag{29}$$

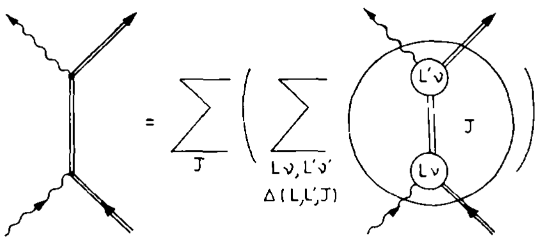

Fig. 3. Decomposition of the scattering amplitude according to angular momentum and parity transfer.

where ν indicates the type of multipole field ($M^0 = \mathrm{E}$ (electric), $M^1 = \mathrm{M}$ (magnetic)):

$$\boldsymbol{A}^{[L],M}(\mathrm{E}; k) = \frac{1}{k}\boldsymbol{\nabla}\times\boldsymbol{A}^{[L],M}(\mathrm{M}; k)\,, \tag{30}$$

$$\boldsymbol{A}^{[L],M}(\mathrm{M}; k) = i^L j_L(kx)\boldsymbol{Y}^M_{L,L}(\hat{\boldsymbol{x}})\,, \tag{31}$$

and R describes the rotation of the quantization axis into the direction of $\boldsymbol{k}$. The convention of Rose [19]) is used for the rotation matrices. Inserting the multipole expansion into eq. (9) and coupling the multipole fields of incoming and outgoing photons one arrives at

$$T^{\mathrm{fi}}_{\lambda'\lambda}(\boldsymbol{k}',\boldsymbol{k}) = (-)^{1+\lambda'+I_\mathrm{f}-M_\mathrm{i}}\sum_{\substack{L,L',J\\M,M'}}(-)^{L+L'}(2J+1)\begin{pmatrix} I_\mathrm{f} & J & I_\mathrm{i}\\ -M_\mathrm{f} & m & M_\mathrm{i}\end{pmatrix}\begin{pmatrix} L & L' & J\\ M & M' & -m\end{pmatrix}$$
$$\times P_J^{L'L\lambda'\lambda}(k',k)D^L_{M,\lambda}(R)D^{L'}_{M',-\lambda'}(R')\,, \tag{32}$$

where

$$P_J^{L'L\lambda'\lambda}(k',k) = \sum_{\nu,\nu'=0,1}\lambda'^{\nu'}\lambda^{\nu}P_J(M^{\nu'}L', M^{\nu}L, k', k)\,, \tag{33}$$

$$P_J(M^{\nu'}L', M^{\nu}L, k', k) = 2\pi(-)^{L+J}(\hat{L}\hat{L}'/\hat{J})$$
$$\times\langle I_\mathrm{f}\|\sum_{l,l'}\int \mathrm{d}^3x\,\mathrm{d}^3y\,[A_{l'}^{[L']}(M^{\nu'}; k', \boldsymbol{x})\times A_l^{[L]}(M^{\nu}; k, \boldsymbol{y})]^{[J]}T_{l'l}(\boldsymbol{x},\boldsymbol{y})\|I_\mathrm{i}\rangle\,. \tag{34}$$

The vector components of the multipole fields are labelled by suffixes l and l'. The spins and projections of initial and final nuclear states have been denoted by I_i, I_f and M_i, M_f, respectively. The rotations R and R' are indicated in fig. 4.

Parity conservation gives the following selection rule

$$P_J(M^{\nu'}L', M^{\nu}L) = 0 \qquad \text{if } (-)^{L'+\nu'+L+\nu} \neq \pi_\mathrm{i}\pi_\mathrm{f}\,, \tag{35}$$

where π_i, π_f denote the parities of initial and final states, respectively.

For later convenience it will be useful to express the different polarizabilities $P_J(M^{\nu'}L', M^{\nu}L)$ in terms of the $P_J^{L'L\lambda'\lambda}$. One easily finds

$$P_J(M^{\nu'}L', M^{\nu}L, k', k) = \tfrac{1}{4}\sum_{\substack{\lambda'=-1,1\\ \lambda=-1,1}}\lambda'^{\nu'}\lambda^{\nu}P_J^{L'L\lambda'\lambda}(k',k)\,. \tag{36}$$

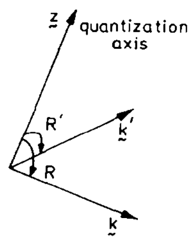

Fig. 4. Scattering geometry and the rotations R and R' carrying the quantization axis into $\boldsymbol{k}$ and $\boldsymbol{k}'$, respectively.

3.1. THE RESONANCE AMPLITUDE

For the resonance amplitude one obtains from (34)

$$P_J^{\text{res}}(M^{\nu'}L', M^{\nu}L, k', k) = 2\pi\hat{L}\hat{L}'(-)^{L-I_f+I_i}$$
$$\times\sum_n\left[\begin{Bmatrix} L & L' & J \\ I_f & I_i & I_n \end{Bmatrix}\frac{\langle I_f\|T_{\nu'}^{[L']}(k')\|I_n\rangle\langle I_n\|T_{\nu}^{[L]}(k)\|I_i\rangle}{E_n-E_i-k-i\varepsilon}\right.$$
$$\left.+(-)^{L+L'+J}\begin{Bmatrix} L' & L & J \\ I_f & I_i & I_n \end{Bmatrix}\frac{\langle I_f\|T_{\nu}^{[L]}(k)\|I_n\rangle\langle I_n\|T_{\nu'}^{[L']}(k')\|I_i\rangle}{E_n-E_i+k'}\right], \tag{37}$$

where the multipole operators $T_{\nu}^{[L]}(k)$ are defined as in ref. [20]) except for an additional i^L factor in order to have simple time-reversal transformation properties so that with a corresponding convention for the wave function the occurring reduced matrix elements become real [see appendix of ref. [20])]. For later purposes we note the following crossing property

$$P_J^{\text{res}}(M^{\nu'}L', M^{\nu}L, k', k) = (-)^J P_J^{\text{res}}(M^{\nu}L, M^{\nu'}L', -k, -k'). \tag{38}$$

Another symmetry relation holds for elastic scattering ($I_f = I_i$) if time-reversal invariance is fulfilled [21])

$$P_J^{\text{res}}(M^{\nu}L, M^{\nu'}L') = P_J^{\text{res}}(M^{\nu'}L', M^{\nu}L). \tag{39}$$

Separating real and imaginary parts of $P_J^{\text{res}}(M^{\nu'}L', M^{\nu}L)$ one has

$$\text{Re}\,(P_J^{\text{res}}(M^{\nu'}L', M^{\nu}L)) = 2\pi\hat{L}\hat{L}'(-)^{L+I_f+I_i}$$
$$\times \text{P}\sum_n\left[\begin{Bmatrix} L & L' & J \\ I_f & I_i & I_n \end{Bmatrix}\frac{\langle I_f\|T_{\nu'}^{[L']}(k')\|I_n\rangle\langle I_n\|T_{\nu}^{[L]}(k)\|I_i\rangle}{E_n-E_i-k}\right.$$
$$\left.+(-)^{L+L'+J}\begin{Bmatrix} L' & L & J \\ I_f & I_i & I_n \end{Bmatrix}\frac{\langle I_f\|T_{\nu}^{[L]}(k)\|I_n\rangle\langle I_n\|T_{\nu'}^{[L']}(k')\|I_i\rangle}{E_n-E_i+k'}\right], \tag{40}$$

where P indicates, that one has to take the principal value, and

$$\text{Im}\,(P_J^{\text{res}}(M^{\nu'}L', M^{\nu}L)) = 2\pi^2\hat{L}\hat{L}'(-)^{L+I_f+I_i}$$
$$\times\sum_n\left[\begin{Bmatrix} L & L' & J \\ I_f & I_i & I_n \end{Bmatrix}\langle I_f\|T_{\nu'}^{[L']}(k')\|I_n\rangle\langle I_n\|T_{\nu}^{[L]}(k)\|I_i\rangle\delta(E_n-E_i-k)\right.$$
$$\left.+(-)^{L+L'+J}\begin{Bmatrix} L' & L & J \\ I_f & I_i & I_n \end{Bmatrix}\langle I_f\|T_{\nu}^{[L]}(k)\|I_n\rangle\langle I_n\|T_{\nu'}^{[L']}(k')\|I_i\rangle\delta(E_n-E_i+k')\right]. \tag{41}$$

It is obvious that the calculation of Im (P_J^{res}) is simplified by the break down of the summation over the intermediate states due to the energy δ-function. The problem arises for the real part of the polarizabilities due to the summation over all intermediate states.

However, the explicit calculation of the real part is relatively simple, if one has to consider only a few resonances as intermediate states like e.g. in the giant resonance region. But for the continuum at higher energies this procedure becomes rather involved and a dispersion theoretical approach is more appropriate. In fact, that has been done implicitly in a recent phenomenological analysis of photon scattering experiments off heavy nuclei above the giant dipole resonance region in approximating the continuum by a superposition of Lorentz lines [12,13]), which obey a dispersion relation.

For the determination of the appropriate dispersion relations for the polarizabilities we will now specialize to elastic scattering, i.e. $k'=k$, and proceed according to ref. [17]) by considering the photon propagator. It differs from the scattering amplitude in the crossing symmetry property, i.e. the imaginary part of the propagator contains an additional $\varepsilon(k)$ factor[†], whereas the real parts are equal. Again it can be expressed in terms of polarizabilities $\tilde{P}_J(k)$, which accordingly differ from $P_J(k)$ by an additional factor $\varepsilon(k)$ in the imaginary part

$$\begin{aligned} \mathrm{Re}\,(P_J^{\mathrm{res}}) &= \mathrm{Re}\,(\tilde{P}_J)\,, \\ \mathrm{Im}\,(P_J^{\mathrm{res}}) &= \varepsilon(k)\,\mathrm{Im}\,(\tilde{P}_J)\,. \end{aligned} \tag{42}$$

Assuming now a dispersion relation for each $\tilde{P}_J(k)$ separately, and using the following crossing relation (cf. eqs. (38), (39))

$$\tilde{P}_J(M^{\nu'}L', M^{\nu}L, -k) = (-)^J\tilde{P}_J^*(M^{\nu'}L', M^{\nu}L, k)\,, \tag{43}$$

one finally arrives at the dispersion relation

$$\mathrm{Re}\,(f(k)-f(0)) = \frac{2k^2}{\pi}\,\mathrm{P}\int \mathrm{d}k'\,\frac{\mathrm{Im}\,f(k')}{k'(k'^2-k^2)}\,, \tag{44}$$

where

$$f(k) = \begin{cases} P_J^{\mathrm{res}}(M^{\nu'}L', M^{\nu}L, k)\,, & \text{for } J = \text{even} \\ (1/k)P_J^{\mathrm{res}}(M^{\nu'}L', M^{\nu}L, k)\,, & \text{for } J = \text{odd}\,. \end{cases} \tag{45}$$

For the latter case (J = odd) one has

$$f(0) = \frac{\mathrm{d}}{\mathrm{d}k}P_J^{\mathrm{res}}|_{k=0}\,. \tag{46}$$

According to these relations we need in addition P_J^{res} and $\mathrm{d}P_J^{\mathrm{res}}/\mathrm{d}k$ at $k=0$ for J even or odd, respectively. For $k\to 0$ the matrix elements behave like

$$\langle n\|T_{\nu}^{[L]}(k)\|\mathrm{i}\rangle \sim k^{L+\nu+1}\,. \tag{47}$$

Therefore the resonance polarizabilities for $k\to 0$ behave like

$$P_J^{\mathrm{res}}(M^{\nu'}L', M^{\nu}L) \sim \begin{cases} k^{L+\nu+L'+\nu'-2}\,, & \text{for } J = \text{even} \\ k^{L+\nu+L'+\nu'-1}\,, & \text{for } J = \text{odd}\,, \end{cases} \tag{48}$$

[†] Recall that $\varepsilon(k) = \pm 1$ for $k \gtrless 0$, respectively.

if there is no ground-state contribution to the intermediate states in eq. (37), otherwise one or two powers less in k for J even or odd, respectively. Then one has

$$P_J^{\rm res}(M^{\nu'}L', M^{\nu}L)|_{k=0} = 0 \qquad \text{for } L+\nu+L'+\nu' > 2\,, \quad (\text{or } 3)\,, \tag{49}$$

and for J odd

$$\frac{\rm d}{{\rm d}k} P_J^{\rm res}(M^{\nu'}L', M^{\nu}L)|_{k=0} = 0 \qquad \text{for } L+\nu+L'+\nu' > 2\,, \qquad (\text{or } 4)\,. \tag{50}$$

The only remaining term is for J even

$$P_{J=0,2}^{\rm res}({\rm E1}, {\rm E1}) = 12\pi(-)^{2I_{\rm i}+1} \sum_{n\neq i} \begin{Bmatrix} 1 & 1 & J \\ I_{\rm i} & I_{\rm i} & I_n \end{Bmatrix} \frac{\langle I_{\rm i}\|E^{[1]}(0)\|I_n\rangle\langle I_n\|E^{[1]}(0)\|I_{\rm i}\rangle}{E_n - E_{\rm i}}\,. \tag{51}$$

Using the Siegert theorem

$$E^{[1]}(0) = -i\frac{1}{\sqrt{6\pi}}[H, D^{[1]}]\,, \tag{52}$$

where $\boldsymbol{D} = \int {\rm d}^3x\, \boldsymbol{x}\rho(\boldsymbol{x})$ is the charge dipole operator, one obtains finally

$$P_{J=0,2}^{\rm res}({\rm E1}, {\rm E1})|_{k=0} = -\frac{1}{\hat{J}}\langle I_{\rm i}\|[D^{[1]}, [H, D^{[1]}]]\|I_{\rm i}\rangle\,, \tag{53}$$

or separately

$$P_0^{\rm res}({\rm E1}, {\rm E1})|_{k=0} = \sqrt{3(2I_{\rm i}+1)}\frac{NZ}{A}\frac{e^2}{M} - \langle I_{\rm i}\|[D^{[1]}, [V, D^{[1]}]]^{[0]}\|I_{\rm i}\rangle\,, \tag{54}$$

$$P_2^{\rm res}({\rm E1}, {\rm E1})|_{k=0} = -\sqrt{\tfrac{1}{5}}\langle I_{\rm i}\|[D^{[1]}, [V, D^{[1]}]]^{[2]}\|I_{\rm i}\rangle\,, \tag{55}$$

since

$$[D^{[1]}, [T, D^{[1]}]]^{[2]} = 0\,. \tag{56}$$

The two expressions in eqs. (54) and (55) describe the low-energy limit of $T^{\rm res}$ in eq. (20) in terms of the scalar and tensor polarizabilities.

For J = odd we have to consider

$$\begin{aligned} &\frac{\rm d}{{\rm d}k} P_1^{\rm res}({\rm E1}, {\rm E1})|_{k=0} \\ &\quad = 12\pi(-)^{2I_{\rm i}+1} \sum_{n\neq i} \begin{Bmatrix} 1 & 1 & 1 \\ I_{\rm i} & I_{\rm i} & I_{\rm i} \end{Bmatrix} \frac{\langle I_{\rm i}\|E^{[1]}(0)\|I_n\rangle\langle I_n\|E^{[1]}(0)\|I_{\rm i}\rangle}{(E_n - E_{\rm i})^2} \\ &\quad = \frac{12\pi}{\sqrt{3}}\langle I_{\rm i}\|[D^{[1]}\times D^{[1]}]^{[1]}\|I_{\rm i}\rangle\,. \end{aligned} \tag{57}$$

Taking the non-relativistic one-body charge density operator the components of the dipole operator commute and thus this term vanishes. This is no longer true if one considers relativistic corrections to $\boldsymbol{D}$ [ref. [22]]. However, we did not consider them in the present treatment. Because of the ground-state contribution for M1 there is furthermore

$$\frac{\mathrm{d}}{\mathrm{d}k} P_1^{\mathrm{res}}(\mathrm{M1},\mathrm{M1})|_{k=0} = 12\pi(-)^{2I_i}\begin{Bmatrix} 1 & 1 & 1 \\ I_i & I_i & I_i \end{Bmatrix}(\langle I_i\|M^{[1]}\|I_i\rangle/k)^2|_{k=0}\,. \tag{58}$$

Using

$$\frac{1}{k}M^{[1]}|_{k=0} = -\frac{1}{\sqrt{6\pi}}\mu^{[1]}\,, \tag{59}$$

where $\mu^{[1]}$ is the magnetic moment operator, one can express eq. (58) in terms of the ground-state magnetic moment,

$$\mu_i = \langle I_i I_i|\mu_0^{[1]}|I_i I_i\rangle\,, \tag{60}$$

and obtain

$$\frac{\mathrm{d}}{\mathrm{d}k} P_1^{\mathrm{res}}(\mathrm{M1},\mathrm{M1})|_{k=0} = (-)^{2I_i}\sqrt{\tfrac{2}{3}(I_i+1)(2I_i+1)/I_i}\,\mu_i^2\,. \tag{61}$$

Another ground-state contribution arises from the center-of-mass motion, which we have neglected because of its smallness [22].

The scalar polarizabilities can also be expressed in terms of the corresponding total multipole cross section $\sigma(M^\nu L)$ for unpolarized photons and no nuclear orientation

$$\begin{aligned}\bar{\sigma}_{\mathrm{tot}} &= \sum_L (\sigma(\mathrm{E}L)+\sigma(\mathrm{M}L)) \\ &= \frac{4\pi}{k}\frac{1}{\hat{I}_i}\sum_L \frac{(-)^{L+1}}{\hat{L}}\,\mathrm{Im}\,(P_0^{\mathrm{res}}(\mathrm{E}L,\mathrm{E}L)+P_0^{\mathrm{res}}(\mathrm{M}L,\mathrm{M}L))\,,\end{aligned} \tag{62}$$

from which follows

$$\mathrm{Im}\,(P_0^{\mathrm{res}}(M^\nu L, M^\nu L, k)) = \frac{k}{4\pi}(-)^{L+1}\hat{L}\hat{I}_i\sigma(M^\nu L, k)\,, \tag{63}$$

and thus the dispersion relation

$$\begin{aligned}&\mathrm{Re}\,(P_0^{\mathrm{res}}(M^\nu L, M^\nu L, k)) - \delta_{\nu 0}\delta_{L0}P_0^{\mathrm{res}}(E1, E1, 0) \\ &\quad = (-)^{L+1}\hat{L}\hat{I}_i\frac{k^2}{2\pi^2}\,\mathrm{P}\int \mathrm{d}k'\,\frac{\sigma(M^\nu L, k')}{k'^2-k^2}\,.\end{aligned} \tag{64}$$

Similarly the higher-order polarizabilities can be expressed by total cross sections for polarized radiation and nuclear orientation [21].

In the following we will use the dispersion relation (44) for the numerical evaluation of the real part of the polarizabilities with the imaginary part given by

(41) as input, provided that the integral converges. This has to be analyzed in every special case. We would like to remark, that for a non-relativistic system the dispersion relations are not strictly valid due to an unphysical cut in the upper k-plane [23–25]. Since that pathology occurs at rather high energy it does not consitute a serious problem for the applications in the energy region we are considering here. Finally we would like to mention that Fano [26]) has considered dispersion relations for the polarizabilities in the special case of E1 radiation.

3.2. THE TWO-PHOTON AMPLITUDE

In the same way one derives the polarizabilities of the two-photon amplitude

$$P_J^{\text{TPA}}(M^{\nu'}L', M^{\nu}L, k', k) = 2\pi(-)^{L+J+1}\frac{\hat{L}\hat{L}'}{\hat{J}}\langle I_f\| \sum_{l'l}\int \mathrm{d}^3x\, \mathrm{d}^3y \times[A_{l'}^{[L']}(M^{\nu'}; k', \boldsymbol{x}) \times A_l^{[L]}(M^{\nu}; k, \boldsymbol{y})]^{[J]} B_{l'l}(\boldsymbol{x}, \boldsymbol{y})\|I_i\rangle\,. \tag{65}$$

Using the symmetry relation for the two-photon operator one easily obtains the relation

$$P_J^{\text{TPA}}(M^{\nu}L, M^{\nu'}L', k, k') = (-)^J P_J^{\text{TPA}}(M^{\nu'}L', M^{\nu}L, k', k)\,. \tag{66}$$

For $(L', \nu') = (L, \nu)$ and $k' = k$ one thus finds the selection rule

$$P_J^{\text{TPA}}(M^{\nu}L, M^{\nu}L, k, k) = 0 \tag{67}$$

for J odd.

We have pointed out in sect. 2, that the two-photon amplitude is related to the charge and current operators by the gauge condition (11). Using this relation we can proceed similarly to the usual derivation of Siegert's theorem for the electric multipole components of the current operator and derive a generalization of this theorem for the two-photon polarizabilities. As for the Siegert theorem we start from the decomposition of the electric multipole field

$$\begin{aligned} \boldsymbol{A}^{[L],M}(E; k, \boldsymbol{x}) &= \frac{i^{L+1}}{k}\sqrt{\frac{L+1}{L}}\,\boldsymbol{\nabla}_x j_L(kx)Y^{[L],M}(\hat{\boldsymbol{x}}) - i^{L+1}\frac{\hat{L}}{\sqrt{L}}j_{L+1}(kx)\boldsymbol{Y}^M_{L,L+1} \\ &= \frac{i}{k}\sqrt{\frac{L+1}{L}}\,\boldsymbol{\nabla}_x C^{[L],M}(\boldsymbol{x}) + \boldsymbol{E}'^{[L]M}(k, \boldsymbol{x})\,, \end{aligned} \tag{68}$$

$$C^{[L],M}(k, \boldsymbol{x}) = i^L j_L(kx)Y^{[L]M}(\hat{\boldsymbol{x}})\,. \tag{69}$$

Then by partial integration and with the gauge condition (11) one obtains

$$\sum_{l,l'} \int \mathrm{d}^3x\, \mathrm{d}^3y\, \nabla_{l'}[C^{[L']}(k',x)\times A_l^{[L]}(M^\nu;k,y)]^{[J]} B_{l'l}(x,y)$$

$$= -i \int \mathrm{d}^3x\, \mathrm{d}^3y\, [C^{[L']}(k',x)\times A_l^{[L]}(M^\nu;k,y)]^{[J]}[\rho(x), j_l(y)]$$

$$= -i[M^{[L']}(k') \stackrel{\times}{,} T_\nu^{[L]}(k)]^{[J]}, \tag{70}$$

i.e. this term can be expressed as a commutator of a charge multipole

$$M^{[L']}(k) = \int \mathrm{d}^3x\, \rho(x) C^{[L']}(k,x), \tag{71}$$

with a transverse multipole $T_\nu^{[L]}$ coupled to rank J. Consequently one obtains for the polarizability

$$P_J^{\mathrm{TPA}}(EL', M^\nu L) = 2\pi(-)^{L+J+1}\frac{\hat{L}\hat{L}'}{\hat{J}}$$

$$\times\left(\frac{i}{k'}\sqrt{\frac{L'+1}{L'}}\langle I_\mathrm{f}\|[M^{[L']}(k') \stackrel{\times}{,} T_\nu^{[L]}(k)]^{[J]}\|I_\mathrm{i}\rangle\right.$$

$$\left.+\langle I_\mathrm{f}\| \int \mathrm{d}^3x\, \mathrm{d}^3y \sum_{l',l}[E_{l'}'^{[L']}(k',x)\times A_l^{[L]}(M^\nu;k,y)]^{[J]} B_{l'l}(x,y)\|I_\mathrm{i}\rangle\right). \tag{72}$$

This facilitates the evaluation of polarizabilities of the two-photon amplitude with at least one electric multipole if one can neglect the second term in (72), i.e. $\boldsymbol{E}'^{[L]}$, as is the case for not too high energies. Because in lowest order the charge density is not influenced by exchange corrections and therefore the one-body density can be used in the charge multipole operators. In particular one has in this limit

$$P_J^{\mathrm{TPA}}(EL', EL) = \frac{2\pi}{kk'}(-)^{L+J}\frac{\hat{L}\hat{L}'}{\hat{J}}\sqrt{\frac{(L'+1)(L+1)}{L'L}}\langle I_\mathrm{f}\|[M^{[L']}(k')$$

$$\stackrel{\times}{,}[H, M^{[L]}(k)]]^{[J]}\|I_\mathrm{i}\rangle. \tag{73}$$

The application of these relations will be discussed elsewhere. Here we will not use them but take the complete explicit expressions for the kinetic and exchange two-photon amplitudes.

We first consider the kinetic two-photon amplitude of eq. (12). Separating out the polarizabilities by some recoupling and using (36) one easily arrives at

$$P_J^{\mathrm{kin}}(M^{\nu'}L', M^{\nu}L) = \tfrac{1}{2}\sqrt{\pi}\,(-)^{L'}\frac{(\hat{L}\hat{L}')^2}{\hat{J}}$$

$$\times \sum_{\substack{n,n' \\ \lambda=\pm1 \\ \lambda'=\pm1}} \lambda^{\nu}\lambda'^{\nu'} i^{n+n'}(\hat{n}\hat{n}')^2 \begin{pmatrix} 1 & n & L \\ -\lambda & 0 & \lambda \end{pmatrix}\begin{pmatrix} 1 & n' & L' \\ \lambda' & 0 & -\lambda' \end{pmatrix}\begin{pmatrix} n & n' & J \\ 0 & 0 & 0 \end{pmatrix}$$

$$\times \begin{Bmatrix} n & n' & J \\ L' & L & 1 \end{Bmatrix} \sum_j \langle I_f \| e_j^2 j_n(kr_j) j_{n'}(k'r_j) Y^{[J]}(\hat{r}_j) \| I_i \rangle \,. \tag{74}$$

The π-exchange two-photon amplitude consists of four different terms corresponding to the graphs (b)–(e) given in fig. 1. The structure of the amplitude is derived in detail in ref. [8]), and we will rewrite here the results in a form being convenient for the decomposition.

Introducing the relative and c.m. coordinates of each nucleon pair

$$\boldsymbol{R}_{j'j} = \tfrac{1}{2}(\boldsymbol{r}_{j'} + \boldsymbol{r}_j)\,, \tag{75}$$

$$\boldsymbol{r}_{j'j} = \boldsymbol{r}_{j'} - \boldsymbol{r}_j\,, \tag{76}$$

the π-exchange two-photon amplitude is given by

$$B^{\pi\mathrm{MEC}}_{\mathrm{fi},\lambda'\lambda} = \frac{f^2 e^2}{m^2} \sum_{j \neq j'} \langle \mathrm{f} |\, \mathrm{e}^{i(\boldsymbol{k}-\boldsymbol{k}')\cdot \boldsymbol{R}_{j'j}} T^0_{j'j} b^{\pi\mathrm{MEC}}_{\lambda'\lambda j'j}(\boldsymbol{r}_{j'j}) | \mathrm{i} \rangle\,, \tag{77}$$

where

$$b^{\pi\mathrm{MEC}}_{\lambda'\lambda j'j}(\boldsymbol{r}_{j'j}) = \sum_{\alpha=1,4} b^{\pi\mathrm{MEC},\alpha}_{\lambda'\lambda j'j}\,, \tag{78}$$

according to the four graphs of figs. 1b-e:

(*i*) *pair–pair current*:

$$b^{\pi\mathrm{MEC},1}_{\lambda'\lambda j'j} = \tfrac{1}{2}\Omega\, \mathrm{e}^{-(i/2)(\boldsymbol{k}+\boldsymbol{k}')\cdot \boldsymbol{r}_{j'j}} J^1(r_{j'j}) \boldsymbol{\varepsilon}'^{*}_{\lambda'} \cdot \boldsymbol{\sigma}_{j'} \boldsymbol{\varepsilon}_{\lambda'} \cdot \boldsymbol{\sigma}_j\,; \tag{79}$$

(*ii*) *pair–π-current*:

$$b^{\pi\mathrm{MEC},2}_{\lambda'\lambda j'j} = -2\Omega\, \mathrm{e}^{-(i/2)\boldsymbol{k}'\cdot \boldsymbol{r}_{j'j}} \boldsymbol{\varepsilon}'^{*}_{\lambda'} \cdot \sigma_{j'} \sigma_j \cdot (\boldsymbol{\nabla}_{j'j} + \tfrac{1}{2} i\boldsymbol{k})$$
$$\times \boldsymbol{\varepsilon}_{\lambda} \cdot \boldsymbol{\nabla}_{j'j} J^2(-\tfrac{1}{2}\boldsymbol{k}, \tfrac{1}{2}\boldsymbol{k}, \boldsymbol{r}_{j'j}) | \mathrm{i} \rangle\,; \tag{80}$$

(*iii*) *π-resonance amplitude*:

$$b^{\pi\mathrm{MEC},3}_{\lambda'\lambda j'j} = 2\Omega\, \mathrm{e}^{(i/2)(\boldsymbol{k}+\boldsymbol{k}')\cdot \boldsymbol{r}_{j'j}} \boldsymbol{\sigma}_{j'} \cdot (\boldsymbol{\nabla}_{j'j} - i\boldsymbol{k}') \boldsymbol{\sigma}_j \cdot (\boldsymbol{\nabla}_{j'j} - i\boldsymbol{k})$$
$$\times \boldsymbol{\varepsilon}'^{*}_{\lambda'} \cdot \boldsymbol{\nabla}_{j'j} \boldsymbol{\varepsilon}_{\lambda} \cdot \boldsymbol{\nabla}_{j'j} J^3_0(\boldsymbol{k}', \boldsymbol{k}, \boldsymbol{r}_{j'j})\,; \tag{81}$$

(*iv*) *π-Thomson amplitude*:

$$b^{\pi\mathrm{MEC},4}_{\lambda'\lambda j'j} = \tfrac{1}{2}\Omega \boldsymbol{\varepsilon}_{\lambda} \cdot \boldsymbol{\varepsilon}'^{*}_{\lambda'}\, \mathrm{e}^{-(i/2)(\boldsymbol{k}+\boldsymbol{k}')\cdot \boldsymbol{r}_{j'j}} \boldsymbol{\sigma}_{j'} \cdot (\boldsymbol{\nabla}_{j'j} - i\boldsymbol{k}')$$
$$\times \boldsymbol{\sigma}_j \cdot (\boldsymbol{\nabla}_{j'j} - i\boldsymbol{k}) J^2_0(\boldsymbol{k}', \boldsymbol{k}, \boldsymbol{r}_{j'j})\,. \tag{82}$$

Here we have introduced the following notations:

$$J^1(r)=\frac{e^{-mr}}{4\pi r}, \tag{83}$$

$$J^2(\boldsymbol{k}',\boldsymbol{k},\boldsymbol{r})=\frac{1}{(2\pi)^3}\int d^3q\,\frac{e^{i\boldsymbol{q}\cdot\boldsymbol{r}}}{((\boldsymbol{q}-\boldsymbol{k}')^2+m^2)((\boldsymbol{q}-\boldsymbol{k})^2+m^2)}, \tag{84}$$

$$J^3(\boldsymbol{k}',\boldsymbol{k},\boldsymbol{r})=\frac{1}{(2\pi)^3}\int d^3q\,\frac{e^{i\boldsymbol{q}\cdot\boldsymbol{r}}}{((\boldsymbol{q}-\boldsymbol{k}')^2+m^2)((\boldsymbol{q}-\boldsymbol{k})^2+m^2)(\boldsymbol{q}^2+m^2)}, \tag{85}$$

$$T^0_{j'j}=\boldsymbol{\tau}_{j'}\cdot\boldsymbol{\tau}_j-\tau^3_{j'}\tau^3_j, \tag{86}$$

$$\Omega=\tfrac{1}{2}(1+P_{j'j})\left(1+\begin{pmatrix}\boldsymbol{\varepsilon}_\lambda\leftrightarrow\boldsymbol{\varepsilon}'^{*}_{\lambda'}\\ \boldsymbol{k}\leftrightarrow-\boldsymbol{k}'\end{pmatrix}\right). \tag{87}$$

The operator $P_{j'j}$ interchanges the particles j' and j. Furthermore, f denotes the πN coupling constant and m the pion mass. Details of the decomposition into polarizabilities are given in appendix A. We will list here only the final result:

$$\begin{aligned}P_J^{\pi\text{MEC}}(M^{\nu'}L',M^{\nu}L)=&-\frac{e^2f^2}{m^2}\frac{(\hat{L}'\hat{L})^2}{4\sqrt{4\pi}\,\hat{J}}\sum_{\substack{\lambda=-1,1\\ \lambda'=-1,1\\ \kappa,\kappa'}}\lambda'^{\nu'}\begin{pmatrix}1&\kappa'&L'\\ \lambda'&0&-\lambda'\end{pmatrix}\lambda^{\nu}\begin{pmatrix}1&\kappa&L\\ -\lambda&0&\lambda\end{pmatrix}\\ &\times\sum_{\substack{l,l',s'\\ n,n',s,\mathscr{L},\mathscr{L}'}}(-)^{\kappa+\kappa'+l'}i^{l+l'}\hat{n}\hat{n}'\hat{s}'\hat{\mathscr{L}}\hat{\mathscr{L}}'(\hat{\kappa}\hat{\kappa}'\hat{l}\hat{l}')^2\\ &\times\begin{pmatrix}l&l'&s'\\0&0&0\end{pmatrix}\begin{pmatrix}\mathscr{L}&l&\kappa\\0&0&0\end{pmatrix}\begin{pmatrix}\mathscr{L}'&l'&\kappa'\\0&0&0\end{pmatrix}\\ &\times\begin{Bmatrix}1&\mathscr{L}&n\\ l&L&\kappa\end{Bmatrix}\begin{Bmatrix}1&\mathscr{L}'&n'\\ l'&L'&\kappa'\end{Bmatrix}\begin{Bmatrix}n&l&L\\ n'&l'&L'\\ s&s'&J\end{Bmatrix}\\ &\times\sum_{j'\neq j}\langle I_f\|T^0_{j'j}j_l(kR_{j'j})j_{l'}(k'R_{j'j})[\Delta^{[s]l'j}_{\mathscr{L}\mathscr{L}'nn'}(\boldsymbol{r}_{j'j})\times Y^{[s']}(\hat{\boldsymbol{R}}_{j'j})]^{[J]}\|I_i\rangle.\end{aligned} \tag{88}$$

The operator $\Delta^{[s]}_{\mathscr{L}\mathscr{L}'nn'}$ describes essentially the polarizability for the two-body system because then one has $\boldsymbol{R}_{12}\equiv0$ and then eq. (88) reduces to

$$\begin{aligned}P_J^{\pi\text{MEC}}(M^{\nu'}L',M^{\nu}L)=&-\frac{e^2f^2}{m^2}\frac{\hat{L}\hat{L}'}{16\pi\hat{J}^2}\\ &\times\sum_{\substack{\lambda=-1,1\\ \lambda'=-1,1\\ \mathscr{L},\mathscr{L}'}}\lambda'^{\nu'}\begin{pmatrix}1&\mathscr{L}'&L'\\ \lambda'&0&-\lambda'\end{pmatrix}\\ &\times\lambda^{\nu}\begin{pmatrix}1&\mathscr{L}&L\\ -\lambda&0&\lambda\end{pmatrix}(-)^{\mathscr{L}+\mathscr{L}'+L+L'}\hat{\mathscr{L}}\hat{\mathscr{L}}'\langle I_f\|T^0_{12}\Delta^{[J]12}_{\mathscr{L}\mathscr{L}'LL'}(\boldsymbol{r}_{12})\|I_i\rangle.\end{aligned} \tag{89}$$

The operator $\Delta^{[s]j'j}_{\mathscr{L}\mathscr{L}'nn'}(\boldsymbol{r}_{j'j})$ consists of four parts corresponding to the graphs (b)–(e) in fig. 1:

$$\Delta^{[s]j'j}_{\mathscr{L}\mathscr{L}'nn'}(\boldsymbol{r}_{ij}) = \sum_{\alpha=1}^{4} \Delta^{[s]j'j;\alpha}_{\mathscr{L}\mathscr{L}'nn'}(\boldsymbol{r}_{ij}) \,. \tag{90}$$

Detailed expressions are given in appendix A.

4. Elastic scattering off the deuteron: results and discussion

We will now apply the foregoing formalism to elastic photon deuteron scattering. We have chosen the deuteron because its bound and continuum wave functions are well known in the non-relativistic framework for a given realistic nucleon–nucleon potential, and they have been tested in many photo- and electrodisintegration processes. The present results have been obtained with the Reid soft-core potential [27]) but other realistic potentials will give very similar results.

According to the previous section the interesting quantities which determine the scattering cross section are the nuclear polarizabilities P_J. They contain information on the dynamical properties of the two-nucleon system. Since the deuteron has spin = 1 one has to consider scalar, vector and tensor polarizabilities ($J = 0, 1, 2$). The scalar polarizability describes the isotropic response to an external electromagnetic field while the vector and tensor polarizabilities are related to optical activity and anisotropy of the system.

With respect to the various multipole combinations of the polarizabilities $P_J(M^{\nu'}L', M^{\nu}L)$ we recall the selection rule with respect to angular momentum conservation $|L-J| \leq L' \leq L+J$. Furthermore, parity conservation requires $L'+\nu'+L+\nu =$ even (see eq. (35)). Thus we have to consider only the following combinations:

scalar: $P_0(\mathrm{E}L, \mathrm{E}L), P_0(\mathrm{M}L, \mathrm{M}L)$,

vector: $P_1(\mathrm{E}L, \mathrm{E}L), P_1(\mathrm{M}L, \mathrm{M}L)$,
$P_1(\mathrm{E}L, \mathrm{M}(L+1)), P_1(\mathrm{M}L, \mathrm{E}(L+1))$,

tensor: $P_2(\mathrm{E}L, \mathrm{E}L), P_2(\mathrm{M}L, \mathrm{M}L)$,
$P_2(\mathrm{E}L, \mathrm{M}(L+1)), P_2(\mathrm{M}L, \mathrm{E}(L+1))$,
$P_2(\mathrm{E}L, \mathrm{E}(L+2)), P_2(\mathrm{M}L, \mathrm{M}(L+2))$.

The remaining polarizabilities $P_J(M^{\nu'}L', M^{\nu}L)$ with $L'>L$ are obtained with the help of the symmetry relations of eqs. (39) and (66). Vector polarizability will only be present in the resonance amplitude due to the selection rule (67) for the two-photon amplitude.

We will first consider the resonance amplitude. The intermediate states will be the partial waves

$$|\mu j m_j\rangle = \sum_{ls} U^{j}_{ls\mu} |\mu (ls) j m_j\rangle \tag{91}$$

of the (incoming) scattering state of the n–p continuum characterized by the momentum $\boldsymbol{p}$

$$|\boldsymbol{p}, sm_s\rangle^{(-)} = \sum_{\mu j m_j l} \frac{\hat{l}}{\sqrt{4\pi}} (l0sm_s|jm_s)\, e^{-i\delta^j_\mu} U^j_{ls\mu} D^j_{m_j m_s}(K^{-1})|\mu j m_j\rangle \tag{92}$$

in the Blatt–Biedenharn convention [28]). The rotation of $\boldsymbol{p}$ into the quantization axis is denoted by K. In the notation of Partovi [29]) one has for the current transition matrix element between ground state and scattering state

$$\langle \boldsymbol{p}, sm_s|j_\lambda(\boldsymbol{k})|m_d\rangle = -c\sqrt{4\pi} \sum_{\substack{Lm\mu\\ ljm_j}} \frac{\hat{l}}{\hat{j}} (1m_dLm|jm_j)$$

$$\times (l0sm_s|jm_j) D^L_{m\lambda}(R) D^j_{m_s m_j}(K) \mathcal{O}^{L\lambda}(\mu jls)\,, \tag{93}$$

where

$$c = \frac{1}{\pi}\sqrt{k/2pM}\,, \tag{94}$$

$$\mathcal{O}^{L\lambda}(\mu jls) = e^{i\delta^j_\mu} U^j_{ls\mu} \sum_{\nu=0,1} \mathcal{M}^{(L)}_\nu(\mu j)\,. \tag{95}$$

In contrast to the expression given by Partovi we here have allowed for an arbitrary orientation of the quantization axis. R describes the rotation of the quantization axis into $\boldsymbol{k}$. Furthermore, one has in the notation of ref. [29])

$$\mathcal{M}^{(L)}_\nu(j\mu) = \begin{cases} \mathcal{J}^{(L)}(j\mu)\,, & \nu = 0\,, \text{ electric} \\ \mathcal{S}^{(L)}(j\mu)\,, & \nu = 1\,, \text{ magnetic}\,. \end{cases} \tag{96}$$

These expressions are related to the reduced multipole matrix elements between the ground state and the partial waves of eq. (91). Projecting out from (93) the partial wave contribution

$$\langle \mu j m_j|j_\lambda(\boldsymbol{k})|m_d\rangle = \sum_{sm_s} \int d\Omega_p \langle \mu j m_j|\boldsymbol{p}sm_s\rangle\langle \boldsymbol{p}sm_s|j(\boldsymbol{k})|m_d\rangle\,, \tag{97}$$

where one reads off eq. (92)

$$\langle \mu j m_j|\boldsymbol{p}sm_s\rangle = \sum_l \frac{\hat{l}}{\sqrt{4\pi}} (l0sm_s|jm_s)\, e^{-i\delta^j_\mu} U^j_{ls\mu} D^{j*}_{m_s m_j}(K)\,, \tag{98}$$

one obtains

$$\langle \mu j m_j|j_\lambda(\boldsymbol{k})|m_d\rangle = -4\pi c(-)^{j-m_j} \sum_{Lm} (\mathcal{J}^{(L)}(\mu j) + \lambda\mathcal{S}^{(L)}(\mu j)) D^L_{m\lambda}(R)\,, \tag{99}$$

and therefore

$$\langle \mu j\|T^{[L]}_\nu\|1\rangle = \frac{2}{\hat{L}}\sqrt{\frac{k}{\pi p M}}\, \mathcal{M}^{(L)}_\nu(\mu j)$$

$$= (-)^{j+L}\langle 1\|T^{[L]}_\nu\|\mu j\rangle\,. \tag{100}$$

With the sum over the intermediate states as an integral over the relative n-p energy $E_{\rm np}$ and a sum over the partial waves

$$\sum_n \to \tfrac{1}{2}M \sum_{j\mu} \int \mathrm{d}E_{\rm np}\, p\,, \tag{101}$$

one obtains finally the polarizabilities from the general expressions of eq. (37) in the form ($k = k'$)

$$\begin{aligned} P_J^{\rm res}(M^{\nu'}L', M^{\nu}L) &= 4k(-)^{L+L'} \sum_{j\mu} (-)^j \begin{Bmatrix} L & L' & J \\ 1 & 1 & j \end{Bmatrix} \\ &\times \int \mathrm{d}E_{\rm np}\, \mathcal{M}_{\nu'}^{(L')}(j\mu) \mathcal{M}_{\nu}^{(L)}(j\mu) \left(\frac{1}{E_{\rm np} + k^2/4AM - E_{\rm b} - k - i\varepsilon} \right. \\ &\left. + \frac{(-)^J}{E_{\rm np} + k^2/4AM - E_{\rm b} + k - i\varepsilon} \right) \\ &+ \text{ground-state contribution}\,. \end{aligned} \tag{102}$$

Here we have denoted the deuteron binding energy by $E_{\rm b}$. The imaginary part is then given by

$$\operatorname{Im} P_J^{\rm res}(M^{\nu'}L', M^{\nu}L) = 4\pi k(-)^{\nu+\nu'} \sum_{j\mu} (-)^j \begin{Bmatrix} L & L' & J \\ 1 & 1 & j \end{Bmatrix} \mathcal{M}_{\nu'}^{(L')}(j\mu) \mathcal{M}_{\nu}^{(L)}(j\mu) \tag{103}$$

which will be used as input for the dispersion relation of eq. (45) in order to calculate the real part as is discussed in sect. 3.

For the calculation of the reduced matrix elements $\mathcal{M}_{\nu}^{(L)}(j\mu)$ we have taken a realistic potential [RSC [27])] to determine the bound- and continuum-state wave functions and have included besides the one-body current density also π-meson exchange currents and NΔ and $\Delta\Delta$ isobar configurations. Multipoles up to $L = 4$ are included and found to be sufficient. Details can be found in refs. [30-32]). We would like to remark that with respect to electric transitions the one-body current contribution is obtained by not using the Siegert theorem. Otherwise the major part of exchange currents would be included without explicit use of the two-body exchange current [32]). The dispersion relations are then evaluated numerically by integrating up to $k = 550$ MeV in order to reach numerical stability.

Fig. 5 shows as an example the input Im $(P_J^{\rm res}(M^{\nu'}L', M^{\nu}L))$ for the most important scalar polarizabilities. Due to the additional energy weighting good convergence is achieved. As already mentioned explicit π-production is not included limiting us to the region below the π-production threshold. Since the π-production channel is dominating the total cross section in the Δ-region this channel will influence the real part of the amplitude even below the π-production threshold as is demonstrated in fig. 6, where we show the average total forward scattering amplitude without

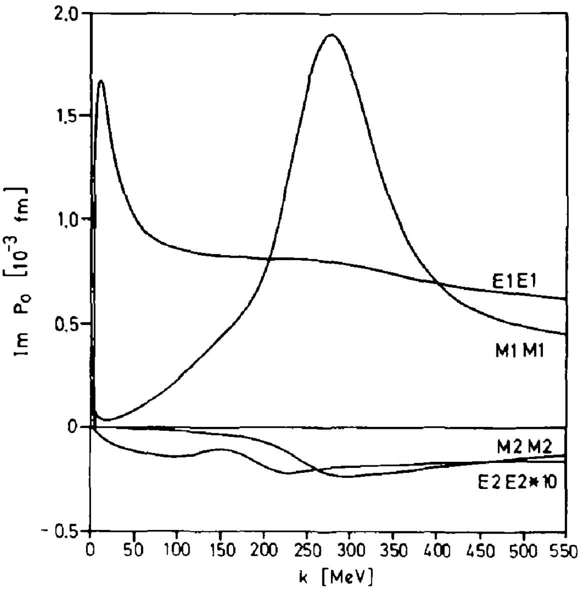

Fig. 5. Imaginary part of the scalar polarizabilities for the lowest multipoles. MEC and IC are included.

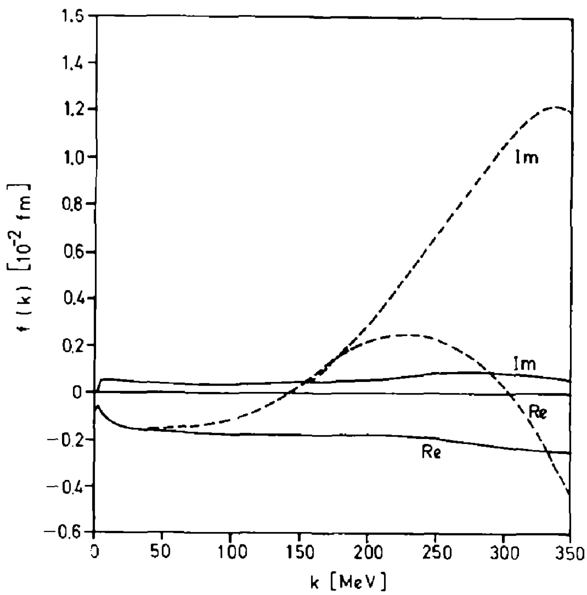

Fig. 6. Real and imaginary parts of the forward scattering amplitude from the optical theorem and dispersion relations. Dashed curves include contributions of real pion production.

and with the contribution of real π-production as taken from ref. [33]) by drawing a smooth curve through the experimental data.

One readily sees the influence on the real part of the amplitude also below the π-production threshold. For our present analysis, however, knowledge of the average total cross section σ_{tot} alone is not sufficient because for the polarizabilities we need the decomposition of σ_{tot} into the various multipole contributions. To this end one has to make a theoretical calculation including real π-production which we do not have available at present; this will be done in the future. Furthermore, for the vector and tensor polarizabilities we would need to know the total cross section for polarized photons and oriented deuterons as discussed in sect. 3. Thus, fig. 6 shows only the contribution of the scalar polarizabilities to the forward scattering amplitude. Neglect of the pion channel will therefore lead to an increasing underestimation of the scattering cross sections when approaching the π-production threshold. But it will still allow us to investigate the relative importance of the ETPA which is the major objective of this study.

Now we will turn to the discussion of the various multipole polarizabilities. Figs. 7–9 show scalar, vector and tensor polarizabilities for both E1 and M1. At low energy, say up to 50 MeV the scalar E1 polarizability is dominating whereas M1 is considerably smaller except near the threshold region. However, while E1 is appreciably reduced at higher energies M1 shows a steady increase which is dramatically enhanced due to the Δ-isobar excitation. Both E1 and M1 show a strong effect of MEC the major part of which is contained in the Siegert operator for E1. Contrary to M1 the IC effects are small for E1 which is not surprising because the dominating NΔ configuration is essentially excited via M1 transition.

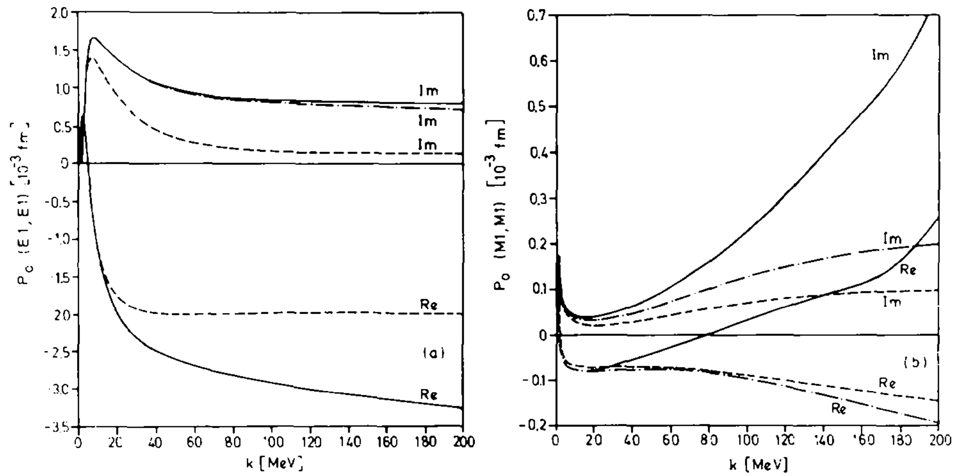

Fig. 7. Scalar polarizabilities for E1(a) and M1 (b). Dashed curves are without MEC (no Siegert theorem) and IC; dash-dot curves include MEC and full curves include MEC and IC. For the real part of E1 the dash-dot and full curves coincide.

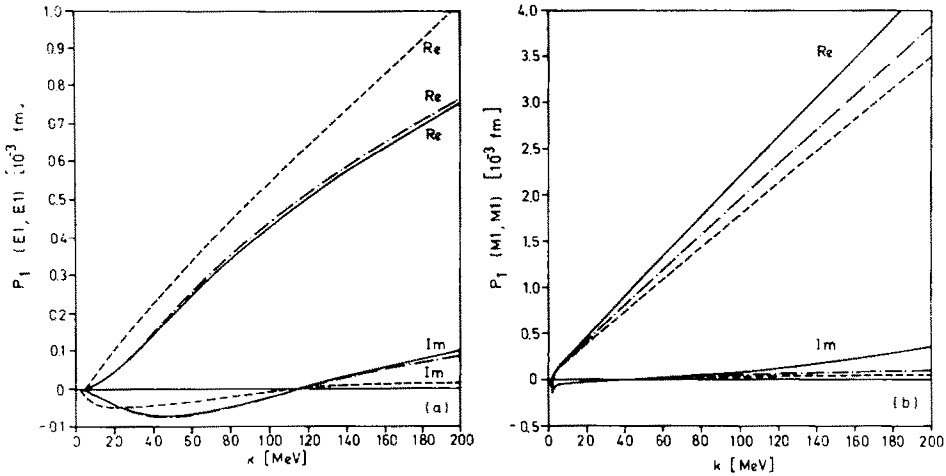

Fig. 8. Vector polarizabilities for E1 (a) and M1 (b). Notation as in fig. 7.

The vector polarizability characterizing the optical activity of the deuteron becomes quite sizeable with increasing energies (fig. 8). Here M1 is clearly dominating over E1. It is interesting to note that exchange effects are much smaller in comparison to the scalar polarizabilities. M1 is slightly increased whereas E1 is somewhat more strongly decreased by MEC. Also the IC show a much smaller effect for both E1 and M1 as well.

The nonvanishing tensor polarizability in fig. 9 reflects the fact that the deuteron is optically anisotropic because of its slight deformation due to the small D-component. Even though the tensor polarizability is much smaller than scalar and

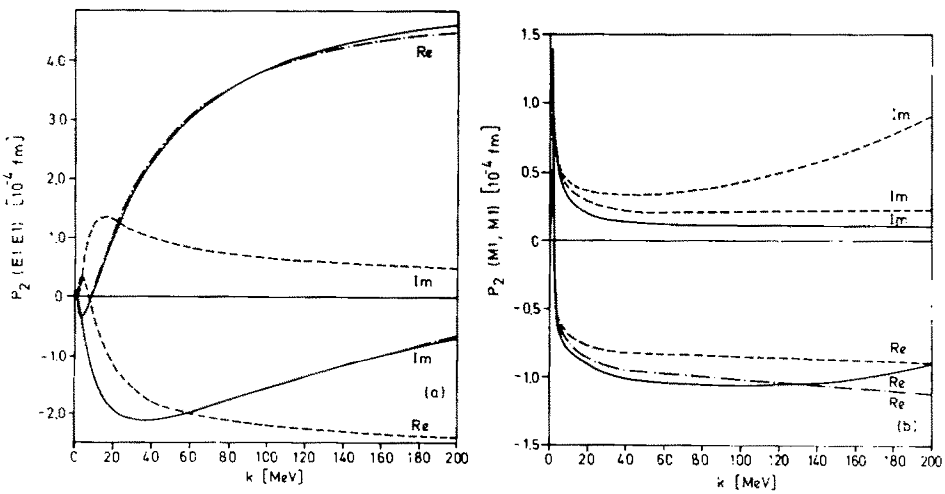

Fig. 9. Tensor polarizabilities for E1 (a) and M1 (b). Notation as in fig. 7.

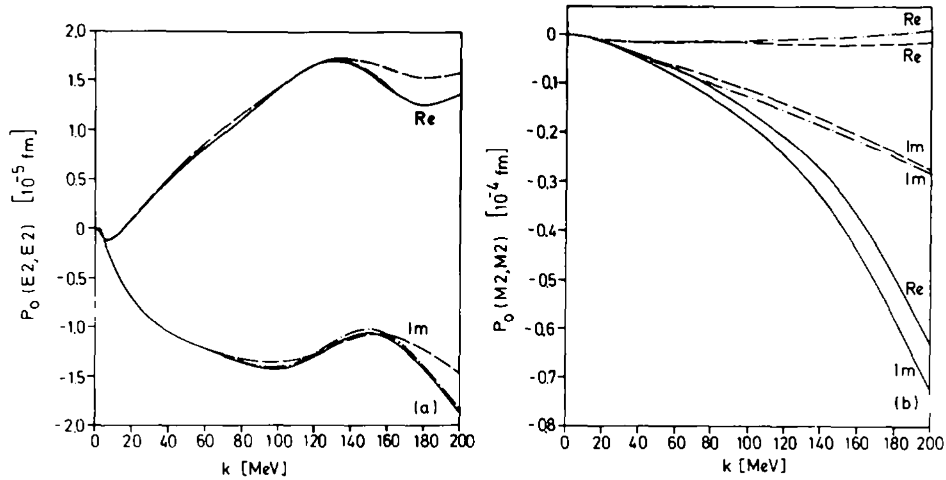

Fig. 10. Scalar polarizabilities for E2 (a) and M2 (b). Notation as in fig. 7.

vector polarizabilities it is remarkable to note the very strong MEC effect in E1 leading even to a sign change. The M1 tensor polarizability is much smaller. Again the IC show a strong influence at higher energies.

The higher multipole polarizabilities decrease rapidly with increasing multipole order. As an example we show the scalar polarizabilities for E2 and M2 in fig. 10. Comparison with fig. 7 shows that they are more than an order of magnitude smaller. E2 is considerably smaller than M2. The latter again has sizeable IC contributions with increasing energy whereas E2 is little affected by exchange effects. Fig. 11 shows the most important mixed (E1, M2) vector polarizability. At higher energies it becomes comparable to the E1 vector polarizability (fig. 8a).

The scalar and tensor polarizability of the two-photon amplitude are shown in figs. 12 and 13 for both the kinetic part and the exchange part. The vector polarizability vanishes as mentioned before. One readily sees that the exchange effects beyond the zero-energy limit (see eq. (19)) are small for the scalar polarizabilities in fig. 12. In contrast to this one observes in fig. 13 a strong enhancement for the pure E1 and M1 tensor polarizabilities. Also the mixed E1–M2 and E2–M1 tensor polarizabilities show a considerable change. However, these relatively large effects in the tenor polarizabilities do not show up in the averaged cross section where the scalar and vector polarizabilities dominate.

At this point we would like to make a remark on the extrapolations of the low-energy expressions to higher photon momenta by Christillin and Rosa-Clot. Their first expression for the ETPA as given in eq. (12) of ref. [6]) (a factor $\frac{1}{3}$ is missing) subtracting the $k=0$ limit leads to a strong underestimation in the deuteron [34,35]), by about a factor 5 for 100 MeV in the forward direction. The second approximation at which the authors arrive after some unclear manipulations

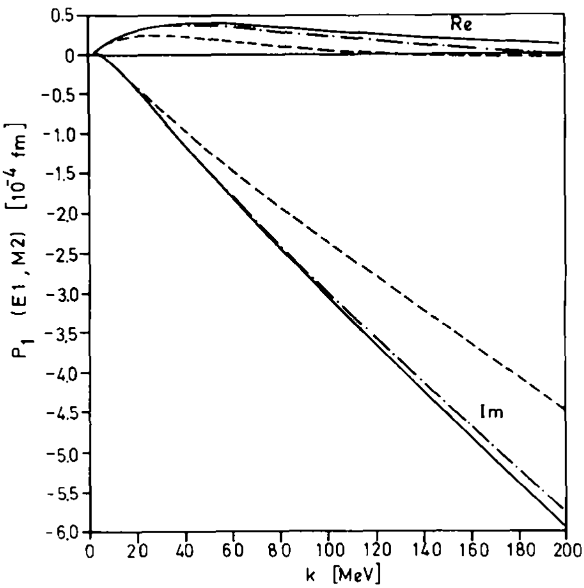

Fig. 11. Vector polarizability for mixed E1–M2. Notation as in fig. 7.

as given in eq. (2) of ref. [7]) gives a constant in the deuteron, i.e. the low-energy limit for all photon momenta. Therefore one cannot expect to obtain any reliable estimate of the size of the ETPA in more complex nuclei using these expressions [36]).

A second remark is concerned with the fourth graph of the π-ETPA (fig. 1e) describing Thomson scattering off exchanged pions. Its amplitude is like the kinetic

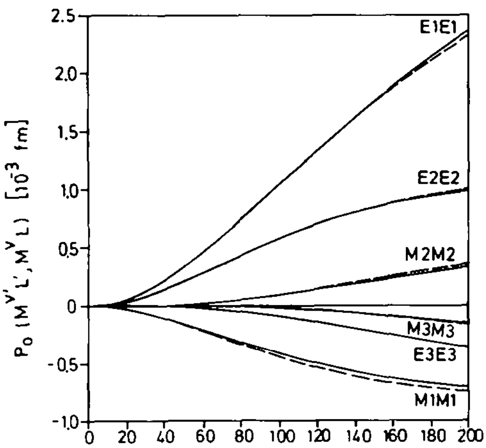

Fig. 12. Scalar polarizabilities of the two-photon amplitude (beyond low-energy limit) for kinetic part only (dashed curves) and with exchange part (full curves).

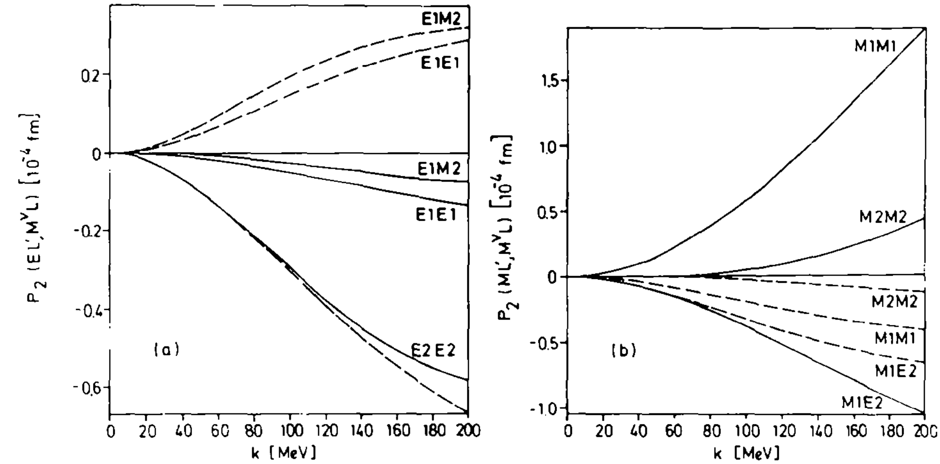

Fig. 13. Tensor polarizabilities of the two-photon amplitude (beyond low-energy limit) for various multipole combinations. Notation as in fig. 12.

TPA a form factor. However, there is an important difference. Because it considers only charged pions exchanged between different nucleons it is not a form factor of a ground-state density but a transition form factor. Therefore one cannot extract from its limit for zero momentum transfer the number of exchanged pions as has been done previously [7,32]). In fact its $q = 0$ limit would give for this quantity (n_π)

$$-(m/e^2)B^{\pi\text{MEC},4}_{\text{ii},\lambda\lambda} = \tfrac{1}{3}(f^2/2\pi)\int_0^\infty \mathrm{d}r\,\{-(2/mr-1)u_\mathrm{S}^2-(1+4/mr)u_\mathrm{D}^2 + 4\sqrt{2}(1+1/mr)u_\mathrm{S}u_\mathrm{D}\}\,\mathrm{e}^{-mr}, \tag{104}$$

where u_S and u_D denote the radial wave functions. Thus the diagonal contributions from S- and D-waves become negative, and only the S-D interference, which dominates, gives a positive contribution.

Now we will discuss the resulting scattering cross section for unoriented deuterons and unpolarized radiation. Fig. 14 shows for selected angles the energy dependence of the cross section. At low energies one sees the typical minimum resulting from destructive interference between resonance and two-photon amplitude. The increase of the cross section with energy at small angles is due to the increasing importance of the vector polarizabilities (see fig. 8). As expected the cross section falls off more rapidly with increasing scattering angles at higher energies because of higher multipole contributions in the resonance amplitude and increasing momentum transfer for the Thomson amplitude. Meson-exchange effects are very large even at rather low energies whereas isobar configurations play a rôle only at higher energies and backward angles. The dominant contribution of meson exchange is in the resonance amplitude while the ETPA beyond the low-energy limit (see eq.

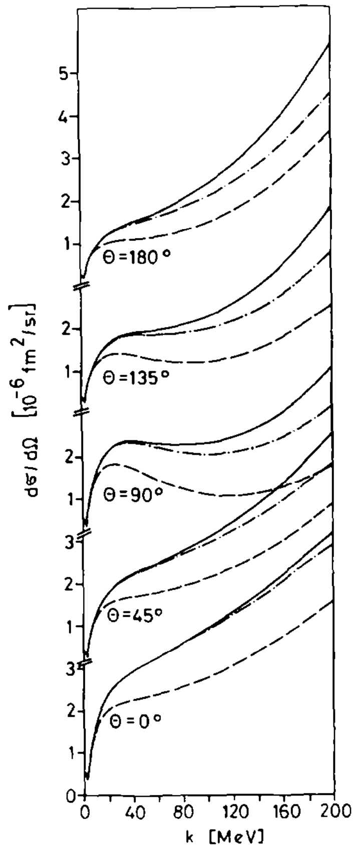

Fig. 14. The differential cross section for unpolarized radiation and unpolarized deuteron versus energy for fixed scattering angles $\theta = 0°$, 45°, 90°, 135° and 180°. Dashed curves without MEC (no Siegert theorem); dash-dot curves include MEC and ETPA contributions; full curves with additional IC contributions.

(19)) is rather small as can be seen in fig. 15 where we have plotted the expected angular distributions at fixed energies. Here we show separately the contribution of the ETPA, and its smallness compared to the other MEC and IC effects is obvious. This is quite in contrast to the early estimates of ref. [7]) predicting a strong effect above the giant resonance region.

Finally, we show in fig. 16 the influence of the vector and tensor polarizabilities on the differential cross section for two energies. It is obvious that with increasing photon energy they become increasingly important. In order to have a comparison with phenomenological approaches we have interpreted the theoretical total absorption cross section (i.e. without real π-production) as pure E1. The resulting angular distribution is quite similar to the one obtained without vector and tensor polarizabilities underlining the dominance of E1 contributions. Furthermore, we

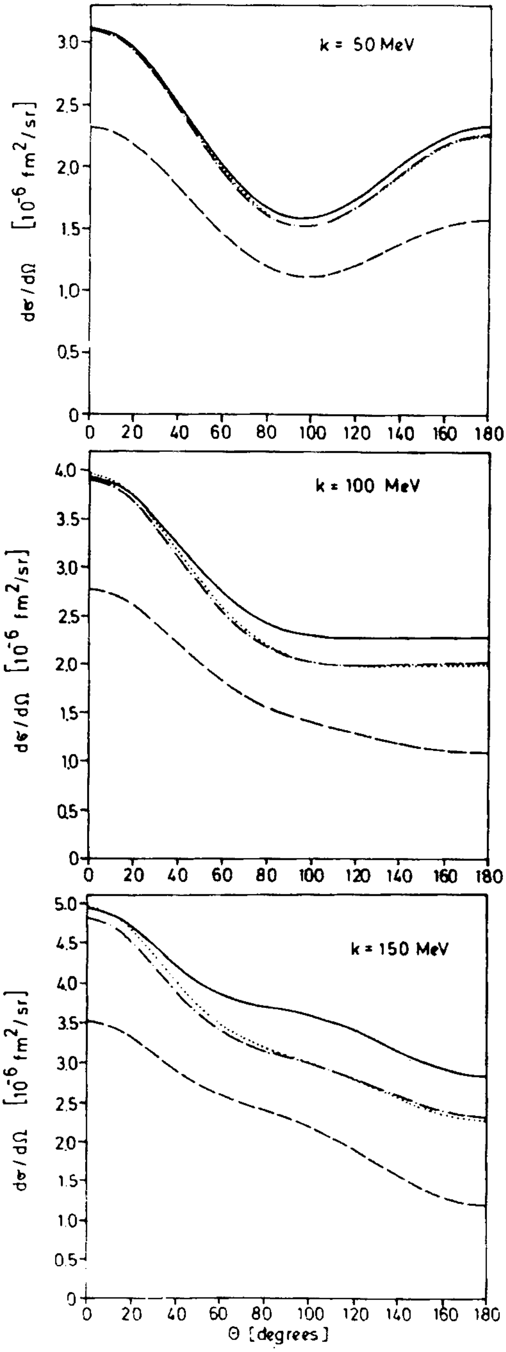

Fig. 15. Angular distributions of the scattering cross section for selected energies (50,100 and 150 MeV) in the Breit system (cf. sect. 2)). Notations as in fig. 14; in addition, dotted curves include only MEC in the resonance amplitude.

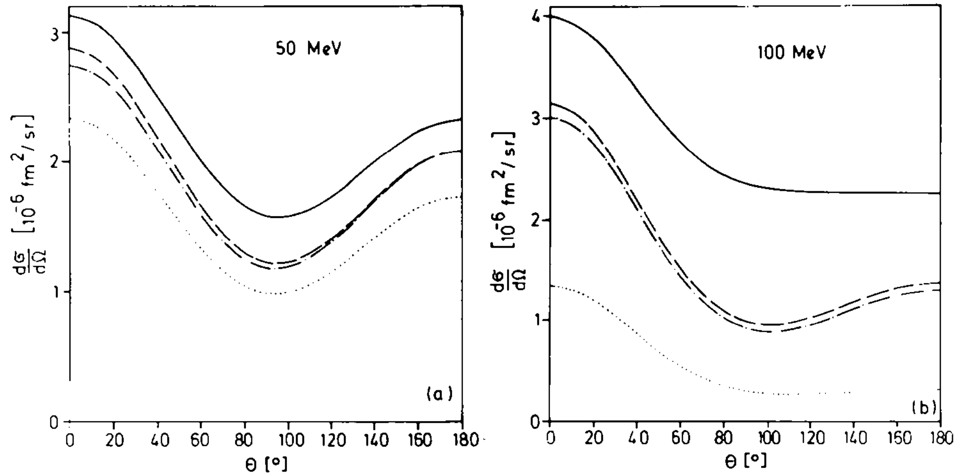

Fig. 16. Angular distributions of the scattering cross section for 50 (a) and 100 MeV (b) photon energy in the Breit system. Full curves: all contributions except ETPA beyond the low-energy limit: dashed curves: without vector and tensor polarizabilities; dash-dot curves: only scalar polarizability assuming the total absorption being E1 only; dotted curves: as dash-dot curves with inclusion of real π-production.

have added to the total cross section the real π-production part interpreting it again as E1, which is certainly not correct in the Δ-region, and arrive at an angular distribution accidentally rather similar to the original one but considerably smaller at 100 MeV.

Thus we can conclude that exchange effects become very important in the resonance amplitude. But the major part is already implicitly contained if the Siegert operator is used for electric transitions. Meson-exchange effects in the TPA are also important to fulfil the low-energy theorem. However, the photon-momentum-dependent part beyond the low-energy limit shows a small effect only in the deuteron. This might be changed to some extent for more complex nuclei having a more pronounced two-body short-range structure.

The investigation of heavier nuclei will be one of the future tasks for which it will be necessary to develop some useful approximations allowing a reliable evaluation of the ETPA because an analogous calculation to the deuteron appears prohibitive. However, it is already evident from the present study that it is not possible to extract a form factor of the charged pion distribution in nuclei. Because of its complicated structure the ETPA amplitude does not depend on the momentum transfer $\boldsymbol{q}$ only but also on $\boldsymbol{k}+\boldsymbol{k}'$. Only the fourth graph, i.e. the Thomson amplitude for an exchanged pion, has the structure of a form factor; however, not a form factor of a ground-state distribution but of a transition distribution according to the exchange character.

Another interesting result is the sizeable vector polarizability related to the dependence on the photon circular polarization of the photoabsorption cross section of oriented deuterons, i.e. to the optical activity of the deuteron. For a quantitative comparison with experiments it is imperative to include the contributions from real π-production which have presently been left out but will be considered in the future. Furthermore, retardation effects for both the exchange current in the resonance amplitude and the ETPA have to be investigated as well as inclusion of isobar contributions in the ETPA. The latter could be particularly interesting for photon scattering in the Δ-region.

We would like to thank W. Leidemann for his help in the calculation of the total photodisintegration cross section.

Appendix A

POLARIZABILITIES OF THE π-ETPA

Here we will present in some detail the decomposition of the π-ETPA into polarizabilities. Instead of using eq. (34) directly we will start from eq. (77):

$$B^{\pi\mathrm{MEC}}_{\mathrm{fi},\lambda'\lambda}=\frac{f^2e^2}{m^2}\sum_{\substack{j\neq j'\\ \alpha=1,4}}\langle \mathrm{f}|T^0_{j'j}\,\mathrm{e}^{i(\boldsymbol{k}-\boldsymbol{k}')\cdot\boldsymbol{R}_{j'j}}b^{\pi\mathrm{MEC},\alpha}_{\lambda'\lambda j'j}(\boldsymbol{r}_{j'j})|\mathrm{i}\rangle\,. \tag{A.1}$$

The different $b^{\pi\mathrm{MEC},\alpha}_{\lambda'\lambda j'j}(\boldsymbol{r}_{j'j})$ are given by eqs. (79)–(82). We will show below that $b^{\pi\mathrm{MEC},\alpha}_{\lambda'\lambda j'j}$ can be brought into the form

$$b^{\pi\mathrm{MEC},\alpha}_{\lambda'\lambda j'j}(\boldsymbol{r}_{j'j})=\sum_{\mathscr{L},\mathscr{L}',n,n',s}[\Gamma^{[s]}_{\lambda\lambda'\mathscr{L}\mathscr{L}'nn'}\times\Delta^{[s]jj',\alpha}_{\mathscr{L}\mathscr{L}'nn'}(\boldsymbol{r}_{j'j})]^{[0]}\,, \tag{A.2}$$

with

$$\Gamma^{[s]}_{\lambda\lambda'\mathscr{L}\mathscr{L}'nn'}=[[\varepsilon^{[1]}_{\lambda}\times Y^{[\mathscr{L}]}(\hat{\boldsymbol{k}})]^{[n]}\times[\varepsilon'^{*[1]}_{\lambda'}\times Y^{[\mathscr{L}']}(\hat{\boldsymbol{k}}')]^{[n']}]^{[s]}\,. \tag{A.3}$$

Using the expansion of the plane wave

$$\mathrm{e}^{i(\boldsymbol{k}-\boldsymbol{k}')\cdot\boldsymbol{R}_{j'j}}=(4\pi)^{3/2}\sum_{l,l',s}(-)^{l'}B^{s}_{ll'}(\tfrac{1}{2}kr,\tfrac{1}{2}k'r)$$
$$\times[[Y^{[l]}(\hat{\boldsymbol{k}})\times Y^{[l']}(\hat{\boldsymbol{k}}')]^{[s]}\times Y^{[s]}(\hat{\boldsymbol{R}}_{j'j})]^{[0]}\,, \tag{A.4}$$

$$B^{s}_{ll'}(x,y)=i^{l+l'}C_{ll's}j_l(x)j_{l'}(y)\,,\qquad C_{ll's}=\hat{l}\hat{l}'\hat{s}\begin{pmatrix} l & l' & s\\ 0 & 0 & 0\end{pmatrix}, \tag{A.5}$$

and by some recoupling one obtains for the π-exchange TPA

$$B^{\pi\mathrm{MEC}}_{\mathrm{fi},\lambda'\lambda}=\frac{f^2e^2}{m^2}\sum_{\substack{j\neq j'\\ \alpha=1,4}}\langle \mathrm{f}|T^0_{j'j}\sum_{\substack{\mathscr{L}\mathscr{L}'nn'ss'\\ LL'\kappa\kappa'J}}U^{\mathscr{L}\mathscr{L}'nn'ss'}_{LL'\kappa\kappa'J}(r_{j'j})$$
$$\times[\Gamma^{[J]}_{\lambda\lambda'\kappa\kappa'LL'}\times[\Delta^{[s]j'j}_{\mathscr{L}\mathscr{L}'nn'}\times Y^{[s']}(\hat{\boldsymbol{R}}_{j'j})]^{[J]}]^{[0]}|\mathrm{i}\rangle\,, \tag{A.6}$$

where

$$U_{LL'\kappa\kappa'J}^{\mathscr{L}\mathscr{L}'nn'ss'}(r)=\sqrt{4\pi}\sum_{l,l'}(-)^{l'+L+L'}B_{ll'}^{s'}(\tfrac{1}{2}kr,\tfrac{1}{2}k'r)$$

$$\times C_{\mathscr{L}l\kappa}C_{\mathscr{L}'l'\kappa'}\begin{Bmatrix}1 & \mathscr{L} & n\\ l & L & \kappa\end{Bmatrix}\begin{Bmatrix}1 & \mathscr{L}' & n'\\ l' & L' & \kappa'\end{Bmatrix}\begin{Bmatrix}n & l & L\\ n' & l' & L'\\ s & s' & J\end{Bmatrix}. \tag{A.7}$$

For the extraction of the polarizabilities we use

$$[\varepsilon_\lambda^{[1]}\times Y^{[\kappa]}(\hat{k})]_M^{[L]}=(-)^{\kappa+1}\frac{\hat{\kappa}\hat{L}}{\sqrt{4\pi}}\begin{pmatrix}1 & \kappa & L\\ -\lambda & 0 & \lambda\end{pmatrix}D_{-\lambda,M}^{L}(R^{-1}). \tag{A.8}$$

Inserting this expression into eq. (A.6) one obtains the polarizabilities as given in (88) by comparison with the definitions in (32) and (33).

Our next task is the derivation of eq. (A.2) and the determination of the $\Delta_{\mathscr{L}\mathscr{L}'nn'}^{[s]jj',\alpha}(\boldsymbol{r}_{j'j})$ corresponding to the different $b_{\lambda'\lambda j'j}^{\pi\mathrm{MEC},\alpha}(\boldsymbol{r}_{j'j})$. We will see that the general form will be

$$\Delta_{\mathscr{L}\mathscr{L}'nn'}^{[s]jj',\alpha}=\hat{n}\hat{n}'\hat{s}\sum_{f,g}\tfrac{1}{2}(1+(-)^{f+g})[Z_{\mathscr{L}\mathscr{L}'nn'}^{fgs,\alpha}(k,k',r_{j'j})$$

$$+(-)^{\mathscr{L}+\mathscr{L}'+n+n'+s}Z_{\mathscr{L}'\mathscr{L}n'n}^{fgs,\alpha}(k',k,r_{j'j})]\Omega_{(f,g)j'j}^{[s]}, \tag{A.9}$$

with

$$\Omega_{(f,g),j'j}^{[s]}=[[\sigma_{j'}^{[1]}\times\sigma_j^{[1]}]^{[f]}\times Y^{[g]}(\hat{r}_{j'j})]^{[s]}, \tag{A.10}$$

by multipole expansions with respect to $\boldsymbol{k}$ and $\boldsymbol{k}'$ and by recoupling. For $b_{\lambda'\lambda j'j}^{\pi\mathrm{MEC},1}(\boldsymbol{r}_{j'j})$ this is easily done yielding

$$Z_{\mathscr{L}\mathscr{L}'nn'}^{fgs,1}(k,k',r_{j'j})=\tfrac{1}{2}(4\pi)^{3/2}i^{\mathscr{L}+\mathscr{L}'}\hat{f}C_{\mathscr{L}\mathscr{L}'g}\begin{Bmatrix}1 & 1 & f\\ \mathscr{L} & \mathscr{L}' & g\\ n & n' & s\end{Bmatrix}$$

$$\times j_{\mathscr{L}}(\tfrac{1}{2}kr_{j'j})j_{\mathscr{L}'}(\tfrac{1}{2}k'r_{j'j})J^1(r_{j'j}). \tag{A.11}$$

For the other terms we first need multipole expansions of the functions $J^2(-\frac{1}{2}\boldsymbol{k},\frac{1}{2}\boldsymbol{k},\boldsymbol{r})$, $J^2(\boldsymbol{k}',\boldsymbol{k},\boldsymbol{r})$ and $J^3(\boldsymbol{k}',\boldsymbol{k},\boldsymbol{r})$. The expansions are given by

$$J^2(-\tfrac{1}{2}\boldsymbol{k},\tfrac{1}{2}\boldsymbol{k},\boldsymbol{r})=\frac{2}{\pi}\sum_{L=\mathrm{even}}i^L\hat{L}\Phi_{L,L}^{(0)}(k,r)[Y^{[L]}(\hat{k})\times Y^{[L]}(\hat{r})]^{[0]}, \tag{A.12}$$

$$J^{\mu}(\boldsymbol{k}',\boldsymbol{k},\boldsymbol{r})=\sum_{\alpha,\alpha',L}i^L C_{\alpha\alpha'L}\Lambda_{\mu,L}^{\alpha,\alpha',(0)}(k,k',r)$$

$$\times[[Y^{[\alpha]}(\hat{k})\times Y^{[\alpha']}(\hat{k}')]^{[L]}\times Y^{[L]}(\hat{r})]^{[0]}, \tag{A.13}$$

with

$$\Phi^{(\nu)}_{\sigma,L}(k,r)=\frac{1}{k^2}\int_0^\infty \frac{\mathrm{d}q\, q^\nu}{Z(q,\frac{1}{2}k)} j_\sigma(qr) Q_L(Z(q,\tfrac{1}{2}k)), \tag{A.14}$$

$$\Lambda^{\alpha,\alpha',(\nu)}_{\mu,\sigma}(k,k',r)=\frac{1}{4\sqrt{\pi}\,kk'}\int_{-1}^1 \mathrm{d}x\int_{-1}^1 \mathrm{d}x'\int_0^\infty \mathrm{d}q$$

$$\times\frac{q^\nu P_\alpha(x)P_{\alpha'}(x')j_\sigma(qr)}{(Z(q,k)-x)(Z(q,k')-x')}\frac{1}{(q^2+m^2)^{\mu-2}}, \tag{A.15}$$

$$Z(q,k)=\frac{1}{2qk}(q^2+k^2+m^2). \tag{A.16}$$

The Legendre polynomials of the first and second kind are denoted by $P_L(z)$ and $Q_L(x)$, respectively, and $j_L(x)$ are the spherical Bessel functions as defined in ref. [37]). A method for the numerical evaluation of $\Phi^{(\nu)}_{\sigma,L}$ is given in ref. [38]) [see also ref. [30])]. For the functions $\Lambda^{\alpha,\alpha',(\nu)}_{\mu,\sigma}$ we describe a similar method in appendix B.

Having the above multipole expansions the next problem is to evaluate an operator $\boldsymbol{a}\cdot\boldsymbol{\nabla}_r$ acting on the functions J^2 and J^3. This is solved by recoupling and using the generalized gradient formula

$$[\nabla^{[1]}\times F(r)Y^{[l]}(\hat{r})]^{[J]}=(-)^{l+1}\hat{l}\begin{pmatrix}1 & l & J\\ 0 & 0 & 0\end{pmatrix}\frac{1}{r}\left\{\frac{\mathrm{d}}{\mathrm{d}r}r+\tfrac{1}{2}[l(l+1)-J(J+1)]\right\}$$

$$\times F(r)Y^{[J]}(\hat{r}) \tag{A.17}$$

in conjunction with the following differentiation formulas derived from the well-known differentiation formula for the spherical Bessel functions [37]):

$$\mathcal{O}^{(\pm)}_\sigma \Lambda^{\alpha,\alpha',(\nu)}_{\mu,\sigma}(k',k,r)=\Lambda^{\alpha,\alpha',(\nu+1)}_{\mu,\sigma\pm1}, \tag{A.18}$$

$$\mathcal{O}^{(\pm)}_\sigma \Phi^{(\nu)}_{\sigma,L}(k,r)=\Phi^{(\nu+1)}_{\sigma\pm1,L}, \tag{A.19}$$

with

$$\mathcal{O}^{(+)}_\sigma=-\frac{\mathrm{d}}{\mathrm{d}r}+\frac{\sigma}{r},\qquad \mathcal{O}^{(-)}_\sigma=\frac{\mathrm{d}}{\mathrm{d}r}+\frac{\sigma+1}{r}. \tag{A.20}$$

As result we get

$$\boldsymbol{a}\cdot\boldsymbol{\nabla}\Lambda^{\alpha,\alpha',(0)}_{\mu,\sigma}[[Y^{[\alpha]}(\hat{k})\times Y^{[\alpha']}(\hat{k}')]^{[L]}\times Y^{[\sigma]}(\hat{r})]^{[\tau]}$$

$$=\sum_\rho[[a^{[1]}\times[Y^{[\alpha]}(\hat{k})\times Y^{[\alpha']}(\hat{k}')]^{[L]}]^{[\rho]}\times Y^{[\rho]}(\hat{r})]^{[\tau]}h_{\rho\sigma}\Lambda^{\alpha,\alpha',(1)}_{\mu,\rho} \tag{A.21}$$

with

$$h_{\rho\sigma}=i^{\rho+\sigma+1}\hat{\rho}\begin{pmatrix}1 & \sigma & \rho\\ 0 & 0 & 0\end{pmatrix}. \tag{A.22}$$

Some tedious recoupling then yields for $Z^{fgs,2}_{\mathscr{L}\mathscr{L}'nn'}$

$$Z^{fgs,2}_{\mathscr{L}\mathscr{L}'nn'}(k,k',r_{j'j}) = \frac{4}{\sqrt{\pi}}\sum_{\tau}(-)^{\tau} i^{\tau+\mathscr{L}'}\hat{\tau}\hat{f}C_{\tau\mathscr{L}'g}\begin{Bmatrix}1 & 1 & f\\ \tau & \mathscr{L}' & g\\ n & n' & s\end{Bmatrix} j_{\mathscr{L}'}(\tfrac{1}{2}k'r_{j'j})$$

$$\times\Bigg[-2\begin{pmatrix}1 & n & \tau\\ 0 & 0 & 0\end{pmatrix}\begin{pmatrix}1 & \mathscr{L} & n\\ 0 & 0 & 0\end{pmatrix}\Phi^{(2)}_{\tau,\mathscr{L}}(k,r_{j'j})$$

$$+k\sum_{l=\text{even}}\hat{l}^2\begin{pmatrix}1 & l & \mathscr{L}\\ 0 & 0 & 0\end{pmatrix}\begin{pmatrix}1 & l & \tau\\ 0 & 0 & 0\end{pmatrix}\begin{Bmatrix}1 & l & \mathscr{L}\\ 1 & n & \tau\end{Bmatrix}\Phi^{(1)}_{\tau,l}(k,r_{j'j})\Bigg]. \tag{A.23}$$

The terms $b^{\pi\text{MEC},3}_{\lambda'\lambda j'j}$ and $b^{\pi\text{MEC},4}_{\lambda'\lambda j'j}$ have a very similar form containing the expression

$$\boldsymbol{\sigma}_{j'}\cdot(\boldsymbol{\nabla}_{j'j}-i\boldsymbol{k}')\boldsymbol{\sigma}_j\cdot(\boldsymbol{\nabla}_{j'j}-i\boldsymbol{k})$$

$$=\tfrac{1}{2}[\boldsymbol{\sigma}_{j'}\cdot\boldsymbol{\nabla}_{j'j}\boldsymbol{\sigma}_j\cdot\boldsymbol{\nabla}_{j'j}-2i\boldsymbol{\sigma}_{j'}\cdot\boldsymbol{k}'\sigma_j\cdot\boldsymbol{\nabla}_{j'j}-\boldsymbol{\sigma}_{j'}\cdot\boldsymbol{k}'\sigma_j\cdot\boldsymbol{k}]+\begin{pmatrix}\boldsymbol{k}'\leftrightarrow\boldsymbol{k}\\ \boldsymbol{\sigma}_{j'}\leftrightarrow\sigma_j\end{pmatrix}, \tag{A.24}$$

so that these terms essentially consist of three structurally different expressions. Therefore, we have the structure

$$b^{\pi\text{MEC},3}_{\lambda'\lambda j'j}(\boldsymbol{r}_{j'j})=\Omega\,\mathrm{e}^{-i(\boldsymbol{k}+\boldsymbol{k}')\cdot\boldsymbol{r}_{j'j}}\left[\beta^3_{\lambda'\lambda j'j}+\begin{pmatrix}\boldsymbol{k}'\leftrightarrow\boldsymbol{k}\\ \boldsymbol{\sigma}_{j'}\leftrightarrow\boldsymbol{\sigma}_j\end{pmatrix}\right], \tag{A.25}$$

with

$$\beta^3_{\lambda'\lambda j'j}=\tfrac{1}{2}[\boldsymbol{\sigma}_{j'}\cdot\boldsymbol{\nabla}_{j'j}\boldsymbol{\sigma}_j\cdot\boldsymbol{\nabla}_{j'j}-2i\boldsymbol{\sigma}_{j'}\cdot\boldsymbol{k}'\boldsymbol{\sigma}_j\cdot\boldsymbol{\nabla}_{j'j}-\boldsymbol{\sigma}_{j'}\cdot\boldsymbol{k}'\sigma_j\cdot\boldsymbol{k}]$$
$$\times\boldsymbol{\varepsilon}'^{*}_{\lambda'}\cdot\boldsymbol{\nabla}_{j'j}\boldsymbol{\varepsilon}_{\lambda}\cdot\boldsymbol{\nabla}_{j'j}J^3_0(k',k,r_{j'j}). \tag{A.26}$$

Bringing $\beta^3_{\lambda'\lambda}(\boldsymbol{r}_{j'j})$ first into the form

$$\beta^3_{\lambda'\lambda}(\boldsymbol{r}_{j'j})=\sum_{\substack{\alpha,\alpha',L\\ r,f,\eta,\tau}}A^{rL\tau}_{\alpha\alpha'f\eta}(k,k',r_{j'j})$$
$$\times[[[\varepsilon^{[1]}_{\lambda}\times\varepsilon'^{*[1]}_{\lambda'}]^{[r]}\times[Y^{[\alpha]}(\hat{\boldsymbol{k}})\times Y^{[\alpha']}(\hat{\boldsymbol{k}}')]^{[L]}]^{[\tau]}\times\Omega^{[\tau]}_{(f,\eta),j'j}]^{[0]}, \tag{A.27}$$

and then $b^{\pi\text{MEC},3}_{\lambda'\lambda}(\boldsymbol{r}_{j'j})$ recoupling to the form of eq. (A.2), one arrives after a lengthy calculation at the final result

$$Z^{fgs,3}_{\mathscr{L}\mathscr{L}'nn'}(k,k',r_{j'j})=\sum_{\substack{l,l',a,\\ \alpha,\alpha',L,\\ f,\eta,\tau,\\ r,\mu}}(-)^{a+f+L+\alpha+\alpha'+r}\hat{\tau}\hat{L}\hat{r}\hat{\mu}^2C_{\alpha l\mathscr{L}}C_{\alpha'l'\mathscr{L}'}C_{\eta a g}$$

$$\times\begin{Bmatrix}\eta & a & g\\ s & f & \tau\end{Bmatrix}\begin{Bmatrix}L & a & \mu\\ s & r & \tau\end{Bmatrix}\begin{Bmatrix}\alpha & l & \mathscr{L}\\ \alpha' & l' & \mathscr{L}'\\ L & a & \mu\end{Bmatrix}\begin{Bmatrix}1 & \mathscr{L} & n\\ 1 & \mathscr{L}' & n'\\ r & \mu & s\end{Bmatrix}$$
$$\times B^a_{ll'}(\tfrac{1}{2}kr_{j'j},\tfrac{1}{2}k'r_{j'j})[A^{rL\tau}_{\alpha\alpha'f\eta}(k,k',r_{j'j})$$
$$+(-)^{f+\alpha+\alpha'+L}A^{rL\tau}_{\alpha'\alpha f\eta}(k',k,r_{j'j})], \tag{A.28}$$

$$A^{rL\tau}_{\alpha\alpha' f\eta}(k,k',r_{j'j})=\sum_{i=1}^{3}A^{rL\tau,i}_{\alpha\alpha' f\eta}(k,k',r_{j'j}), \tag{A.29}$$

where we have according to the three terms in eq. (A.24)

$$A^{rL\tau,1}_{\alpha\alpha' f\eta}(k,k',r_{j'j})=i^{\eta}\hat{r}C_{\alpha\alpha' L}C_{\eta\tau f}\begin{pmatrix}L&\tau&r\\0&0&0\end{pmatrix}\begin{pmatrix}1&1&r\\0&0&0\end{pmatrix}$$

$$\times\begin{pmatrix}1&1&f\\0&0&0\end{pmatrix}A^{\alpha,\alpha',(4)}_{3,\eta}(k,k',r_{j'j}), \tag{A.30}$$

$$A^{rL\tau,2}_{\alpha\alpha' f\eta}(k,k',r_{j'j})=\tfrac{2}{3}ki^{\eta}(-)^{\tau+f+\alpha'}\hat{\tau}\hat{f}\hat{L}\begin{pmatrix}1&1&r\\0&0&0\end{pmatrix}$$

$$\times\sum_{\beta,\kappa,c}C_{\beta\alpha'\kappa}C_{c\kappa r}C_{1\eta c}C_{1\alpha\beta}\begin{Bmatrix}1&1&f\\\tau&\eta&c\end{Bmatrix}\begin{Bmatrix}\kappa&1&L\\\tau&r&c\end{Bmatrix}$$

$$\times\begin{Bmatrix}\beta&1&\alpha\\L&\alpha'&\kappa\end{Bmatrix}A^{\beta,\alpha',(3)}_{3,\eta}(k,k',r_{j'j}), \tag{A.31}$$

$$A^{rL\tau,3}_{\alpha\alpha' f\eta}(k,k',r_{j'j})=\tfrac{1}{3}kk'i^{\eta}(-)^{f}\hat{\tau}\hat{f}\hat{L}\begin{pmatrix}1&1&r\\0&0&0\end{pmatrix} \tag{A.32}$$

$$\times\sum_{\beta,\beta',\kappa}C_{\beta\beta'\kappa}C_{\eta\kappa r}C_{1\alpha\beta}C_{1\alpha'\beta'}\begin{Bmatrix}\kappa&f&L\\\tau&r&\eta\end{Bmatrix}$$

$$\times\begin{Bmatrix}\beta&1&\alpha\\\beta'&1&\alpha'\\\kappa&f&L\end{Bmatrix}A^{\beta,\beta',(2)}_{3,\eta}(k,k',r_{j'j}). \tag{A.33}$$

The corresponding expressions for $Z^{fgs,4}_{\mathscr{L}\mathscr{L}'nn'}$ are obtained by setting $r=0$ in the above results for $Z^{fgs,3}_{\mathscr{L}\mathscr{L}'nn'}$ and by replacing

$$A^{\alpha,\alpha',(\nu)}_{3,\eta}(k,k',r_{j'j})\to-\tfrac{3}{4}A^{\alpha,\alpha',(\nu-2)}_{2,\eta}(k,k',r_{j'j}) \tag{A.34}$$

in every $A^{rL\tau,i}_{\alpha\alpha' f\eta}$ above.

Appendix B

NUMERICAL EVALUATION OF THE FUNCTIONS $A^{\alpha,\alpha',(\nu)}_{\mu r}$

The starting point is eq. (A.15) which can be rearranged since one has according to eqs. (A.30)–(A.32) the selection rule $\alpha+\alpha'+\sigma+\nu=$ even:

$$A^{\alpha,\alpha',(\nu)}_{\mu,\sigma}(k,k',r)=\frac{1}{8\sqrt{\pi}\,kk'}\int_{-1}^{1}\mathrm{d}x\,P_{\alpha}(x)\int_{-1}^{1}\mathrm{d}x'\,P_{\alpha'}(x')$$

$$\times\int_{-\infty}^{\infty}\frac{\mathrm{d}q\,q^{\nu}h^{(1)}_{\sigma}(qr)(q^2+m^2)^{2-\mu}}{(Z(q,k)-x)(Z(q,k')-x')}, \tag{A.35}$$

where we have introduced the spherical Hankel functions of the first kind as defined in ref. [37]). The q-integral can now be done analytically using complex contour integration with the result

$$\Lambda^{\alpha,\alpha',(\nu)}_{\mu,\sigma}=\frac{\sqrt{\pi}}{4kk'}\int_{-1}^{1}\mathrm{d}x\,P_{\alpha}(x)\int_{-1}^{1}\mathrm{d}x'\,P_{\alpha'}(x')\lambda^{(\nu)}_{\mu,\sigma}(x,x')\,, \tag{A.36}$$

where we have introduced

$$\lambda^{(\nu)}_{\mu,\sigma}(x,x')=\frac{kp_1^{\nu+1}h^{(1)}_{\sigma}(p_1r)}{p_1'(Z(p_1,k)-x')(p_1^2+m^2)^{\mu-2}}+\frac{k'p_2^{\nu+1}h^{(1)}_{\sigma}(p_2r)}{p_2'(Z(p_2,k')-x)(p_2^2+m^2)^{\mu-2}}$$
$$+\frac{\delta_{\mu,3}}{2m}\frac{(im)^{\nu}h_{\sigma}(imr)}{(Z(im,k)-x)(Z(im,k')-x')}\,, \tag{A.37}$$

$$p_1=xk+ip_1'\,,\qquad p_1'=\sqrt{k^2(1-x^2)+m^2}\,, \tag{A.38}$$

$$p_2=x'k'+ip_2'\,,\qquad p_2'=\sqrt{k'^2(1-x'^2)+m^2}\,. \tag{A.39}$$

The remaining integrals over x and x' are done by a numerical Gauss integration. It has been proved advantageous to change the variables in the following way instead of integrating directly in the variables x and x':

$$\int_{-1}^{1}\mathrm{d}x\int_{-1}^{1}\mathrm{d}x'\,\lambda^{(\nu)}_{\mu\sigma}(x,x')P_{\alpha}(x)P_{\alpha'}(x')$$
$$=\int_{0}^{2}\mathrm{d}b\int_{-1+b}^{1}\mathrm{d}x\,\lambda^{(\nu)}_{\mu\sigma}(x,-x+b)P_{\alpha}(x)P_{\alpha}(-x+b)$$
$$+\int_{-2}^{0}\mathrm{d}b\int_{-1}^{1+b}\mathrm{d}x\,\lambda^{(\nu)}_{\mu\sigma}(x,-x+b)P_{\alpha}(x)P_{\alpha'}(-x+b)\,. \tag{A.40}$$

We have chosen 16 Gauss points for the numerical integrations in both variables b and x.

In order to test the convergence of the multipole decomposition of $J^2(\boldsymbol{k}',\boldsymbol{k},\boldsymbol{r})$ as well as the numerical calculation of the $\Lambda^{\alpha,\alpha',(\nu)}_{2,\sigma}$ functions) we have considered the specific case $\mathrm{e}^{(i/2)(\boldsymbol{k}+\boldsymbol{k}')\cdot\boldsymbol{r}}J^2(\boldsymbol{k},\boldsymbol{k}',\boldsymbol{r})$ for $\boldsymbol{k}=\boldsymbol{k}'$, for which a simple analytic expression exists:

$$\mathrm{e}^{-i\boldsymbol{k}\cdot\boldsymbol{r}}J^2(\boldsymbol{k},\boldsymbol{k},\boldsymbol{r})=\frac{1}{8\pi m}\mathrm{e}^{\;\;mr}\,, \tag{A.41}$$

independent of $\boldsymbol{k}$. It is found that taking multipoles into account up to $\alpha=\alpha'=L=4$ the agreement between numerical and analytical result is better than 0.5%, if we choose $k=100$ MeV in the numerical evaluation. Corresponding checks have been done for $J^3(\boldsymbol{k},\boldsymbol{k},\boldsymbol{r})$.

References

1) R. Moreh, Proc. Int. School of intermediate energy nuclear physics, ed. R. Bergère, S. Costa and C. Schaerf (Singapore, 1982), p. 1
2) H. Arenhövel, Proc. Int. Conf. on photonuclear reactions and applications, ed. B. L. Berman (Univ. of California, Livermore, 1973) p. 449
3) A. Molinari, Phys. Reports **64C** (1980) 283
4) J.L. Friar, Ann. of Phys. **95** (1975) 170
5) J.L. Friar, Phys. Rev. Lett. **36** (1980) 129
6) P. Christillin and M. Rosa-Clot, Nuovo Cim. **28A** (1975) 29
7) P. Christillin and M. Rosa-Clot, Nuovo Cim. **43A** (1978) 172
8) H. Arenhövel, Z. Phys. **A297** (1980) 129
9) M. Rho and D.H. Wilkinson, ed., Mesons in nuclei (North-Holland, Amsterdam, 1979)
10) H. Arenhövel, Nucl. Phys. **A374** (1982) 521c
11) A. Cambi *et al.*, Nuovo Cim. **47A** (1978) 421
12) R. Leicht *et al.*, Nucl. Phys. **A362** (1981) 111
13) M. Sanzone-Arenhövel *et al.*, Proc. Int. School of intermediate energy nuclear physics, ed. R. Bergère, S. Costa and C. Schaerf (Singapore, 1982) p. 291
14) J.L. Friar and M. Rosen, Ann. of Phys. **87** (1974) 289
15) H. Arenhövel, M. Danos and W. Greiner, Phys. Rev. **157** (1967) 1109
16) H. Arenhövel and W. Greiner, Prog. Nucl. Phys. **10** (1969) 167
17) M. Gell-Mann, M.L. Goldberger and W. Thirring, Phys. Rev. **95** (1954) 1612
18) R. Silbar and H. Überall, Nucl. Phys. **A109** (1968) 146
19) M.E. Rose, Elementary theory of angular momentum (Wiley, New York, 1957)
20) T. DeForest and J.D. Walecka, Adv. of Phys. **15** (1966) 1
21) H. Arenhövel, Phys. Rev. **171** (1968) 1212
22) J.L. Friar, Phys. Rev. **C16** (1977) 1504
23) T. Matsuura and K. Yazaki, Phys. Lett. **46B** (1973) 17
24) J.L. Friar and S. Fallieros, Phys. Rev. **C11** (1975) 274, 277
25) H.P. Schröder and H. Arenhövel, Z. Phys. **A280** (1977) 349
26) U. Fano, NBS Technical Note 83 (1960), reprinted in Photonuclear reactions, ed. E.G. Fuller and E. Hayward (Dowden, Hutchinson & Ross, 1976) p. 338
27) R.V. Reid, Ann. of Phys. **50** (1968) 411
28) J.M. Blatt and L.C. Biedenharn, Phys. Rev. **86** (1952) 399
29) F. Partovi, Ann. of Phys. **27** (1964) 79
30) W. Fabian and H. Arenhövel, Nucl. Phys. **A258** (1976) 461
31) W. Fabian and H. Arenhövel, Nucl. Phys. **A314** (1979) 253
32) H. Arenhövel, Z. Phys. **A302** (1981) 25
33) T.A. Armstrong *et al.*, Nucl. Phys. **B41** (1972) 445
34) M. Weyrauch, Diploma thesis (Mainz, 1980)
35) H. Arenhövel, Lecture Notes in Physics, vol. 137 (1981) p. 136
36) W.M. Alberico and A. Molinari, Z. Phys. **A309** (1982) 143
37) M. Abramowitz and I.A. Stegun, Handbook of mathematical functions (Dover, New York, 1965)
38) W. Leidemann, Diploma thesis (Mainz, 1980)